FAULT INDUCED SUBSIDENCE NEAR EMPIRE

AND BASTIAN BAY, LOUISIANA

A THESIS

SUBMITTED ON THE FIRST DAY OF DECEMBER 2006

TO THE DEPARTMENT OF EARTH AND ENVIRONMENTAL SCIENCES

IN PARTIAL FULFILLMENT OF THE REQUIREMENTS

OF THE SCHOOL OF SCIENCE AND ENGINEERING

OF TULANE UNIVERSITY

FOR THE DEGREE

OF

MASTER OF SCIENCE

BY

Emily Martin

APPROVED:

Nancye Dawers, Ph.D.

Mead Allison, Ph.D.

Suzanne Leclair, Ph.D.

CHAPTER 1: STUDY AREA

Introduction

Rapid subsidence of south Louisiana has long been recognized based on geomorphic and archeological evidence (e.g., Fisk, 1944). More recent geodetic studies suggest as much as 5 to15 mm/yr of present day vertical motion (e.g., Jurkowski et al., 1984; Sella et al., 2005; Dokka, 2005, 2006; Shinkle 2004), whereas Late Pleistocene to Holocene geologic data suggest lower rates (e.g., Saucier, 1963; Kulp and Howell, 2000; Tornqvist et al., 2006). A number of natural and anthropogenic feedbacks are likely to contribute to subsidence (e.g., Gagliano et al., 1981; Gagliano, 1999; Autin, 1993; Kuecher et al., 2001; Morton et al., 2002), and are possibly accelerating it. However, over the last several years, the role of subsidence related to faulting has been increasingly recognized as an important, but poorly understood, process in coastal Louisiana.

This thesis examines the relationship between previously recognized regional normal faults and recent subsidence near Empire, Louisiana (Fig 1.1). Motivation for this project comes from the observation that patterns of marsh loss near both Bastian Bay and the town of Empire in lower Plaquemines Parish, southeast Louisiana (Fig 1.1) suggest en echelon fault segments. Empire lies east of the complex Golden Meadow fault, which also exhibits evidence of fault-bounded recent subsidence (e.g., Keucher et al., 2001).

Anthropogenic mechanisms, such as fluid withdrawal, have recently been proposed as possible initiators of the recent activity along some portions of the Golden Meadow fault (Morton et al., 2001). While there is some correlation between subsidence

along fault lines and times of locally extensive hydrocarbon withdrawal (e.g., White et al., 1997; Morton et al., 2002), and while it is understood how fluid withdrawal can lead to local subsidence (e.g., Bou-Rabee, 1994; Serebryakov et al., 2000,), how withdrawing fluids actually re-activates a large fault is less clear. Additionally, while influences from nearby oil and gas activity may play some role in the faulting regionally, the subsidence at Empire and Bastian Bay does not directly correlate with areas of withdrawal and therefore other mechanisms need to be examined (Fig 1.2).

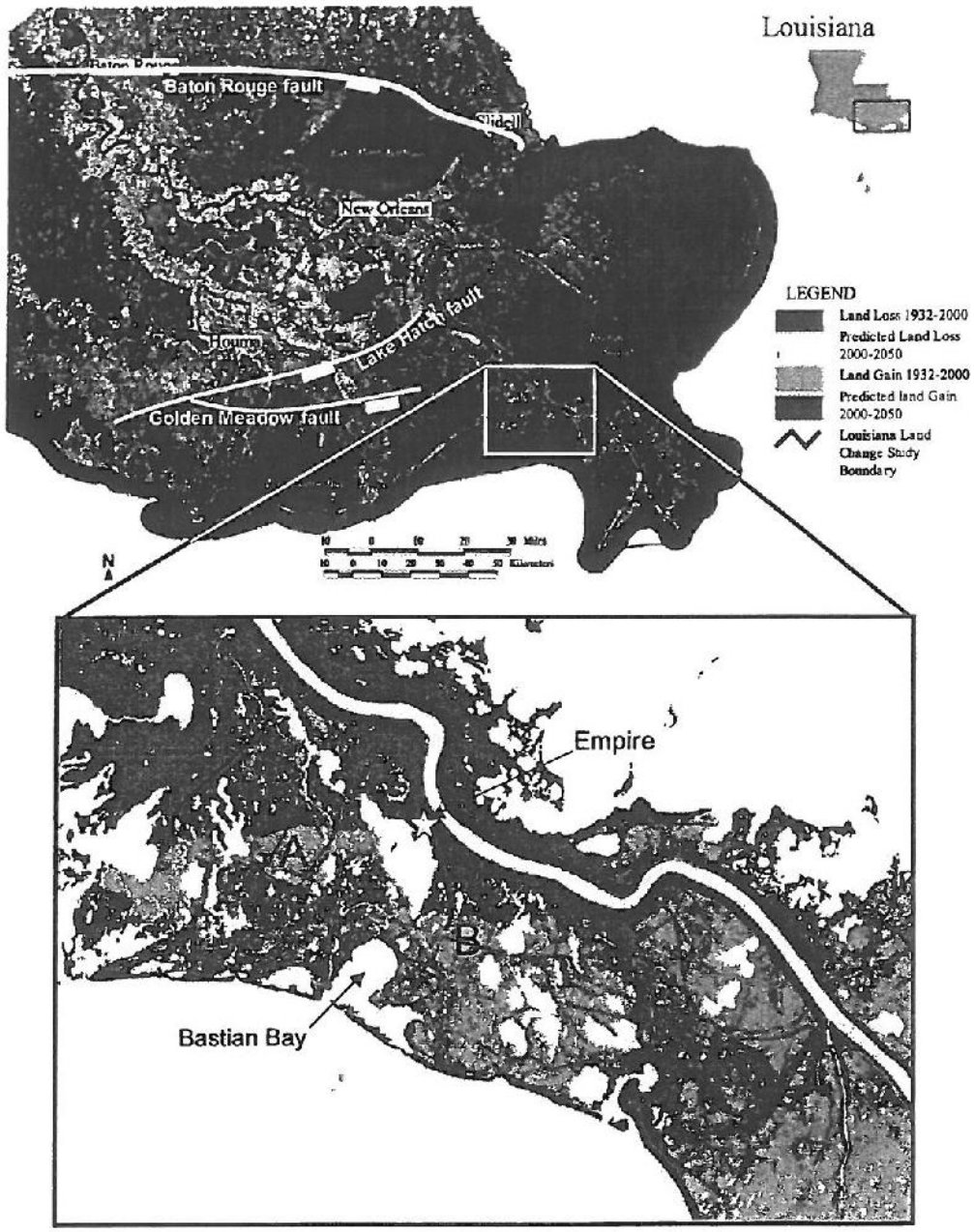

Figure 1.1. Location of the Empire (A) and Bastian Bay (B) marsh breaks within the context of the Golden Meadow and Lake Hatch fault systems of southeastern Louisiana. Historical land loss is broken down by years (USGS, 2003). In the inset, recent land loss is delineated by type, with yellow being interior ponding, red being shoreline gulf, light blue being shoreline lake, dark blue being shoreline bay, and pink being shoreline channel. Green is the current land remaining as of 1990 (USGS, 2001).

Approach

To determine whether observed marsh breaks and recent subsidence west of Empire, Louisiana (area "A" in Figure 1.1) -- which resulted in the creation of a new body of water called "No man's Land" -- and to the south of Empire near Bastian Bay, Louisiana (area "B" in Figure 1.1) are the result of faulting, this study first examines the surface data. These structures are prime candidates for study, as preliminary data identified them as likely having historic displacement (Gagliano et al., 2003a). Using aerial photographs the marsh breaks are divided up into hypothesized fault segments.

Evidence for shallow displacement along the Empire marsh break is then examined using shallow core stratigraphy taken at various intervals across the marsh break with a McCauley Auger. Clear displacement of unit contacts may indicate faulting. Variations within this displacement can aid in defining the length of a fault or a given fault segment (Fig 1.3). Radiocarbon dates taken from samples obtained from the surface cores are utilized to bracket the age of the near-surface sediments. Bathymetric profiles, taken perpendicular to the marsh breaks, record any pattern of subsidence that might be indicative of a fault deformation zone.

The surface data, while consistent with the hypothesis that these marsh breaks are the result of faulting, and further consistent with the hypothesized segment placement, is not conclusive. Motivated by these field observations, a range of subsurface data is examined. The subsurface data, which includes electrical well logs and 2D seismic reflection lines (on paper), is used to more conclusively determine whether the marsh breaks and surrounding subsidence are the result of faulting. Once faults correlating to the surface features and surface data at both Empire and Bastian Bay are positively

identified, these faults are then examined in detail to determine their size, structure, and kinematic history.

The faults identified in this study (hereafter referred to as the "Empire fault" and the "Bastian Bay fault") are then compared to available previously mapped subsurface faults, both within, and tangent to, the immediate study area (Meltzer, 1966; Sabate, 1968). As both the surface and subsurface data also suggest that the Empire and Bastian Bay faults continued eastward, I also describe results obtained from a digital grid of proprietary 2D seismic data, which lies offshore east of the Mississippi River and at roughly the same latitude as the Empire and Bastian Bay fault segments (Figure 1.7).

The various datasets are summarized in Figure 1.6. The surface data and its interpretations are described in further detail in Chapter 2. All subsurface data methods and related correlation and interpretation are described in Chapter 3.

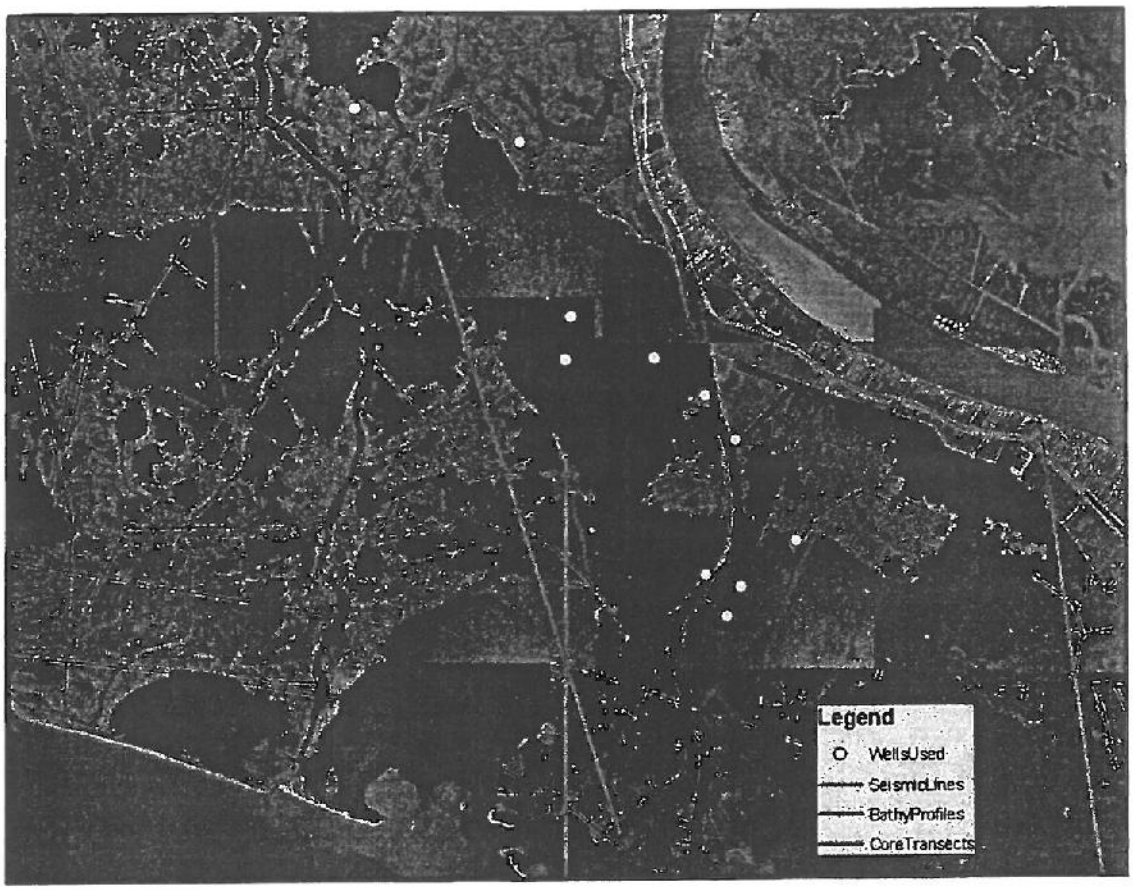

Figure 1.6. Location of various data used in this study in the immediate vicinity of Empire and Bastian Bay.

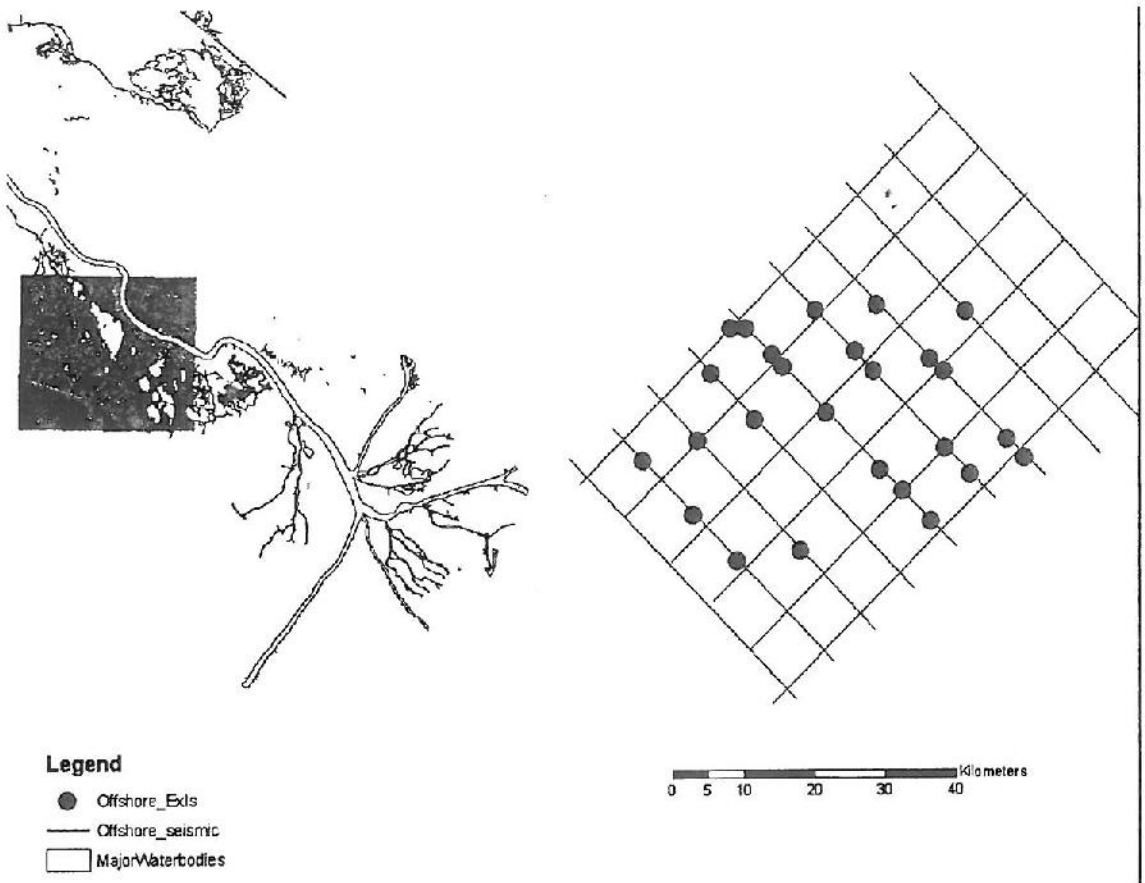

Figure 1.7. Location of the offshore seismic grid relative to the Empire field area. The red dots indicate where data was gathered on large, south dipping faults that disrupt sediments at or very near the present-day seafloor.

CHAPTER 2: SURFACE EXPRESSIONS OF FAULTING IN "NO MAN'S LAND" NEAR EMPIRE, LOUISIANA

Introduction

On land loss maps of southern Louisiana (Penland et. al., 2000), some marsh breaks follow slightly arcuate linear patterns (see inset in Figure 1.1). Such patterns seen in the marsh breaks near both Empire and Bastian Bay, Louisiana suggest the presence of faults, with areas of recent land loss on the down-dropped sides of the faults. We have interpreted possible fault segments along these marsh breaks based on the local geomorphology using LIght Detection And Ranging (LIDAR) imagery, acquired by the Federal Emergency Management Agency and the State of Louisiana through the Louisiana Oil Spill Coordinator's Office (http://atlas.lsu.edu/central/la_lidar_ project.pdf).

There are known geomorphic patterns associated with surface expressions of faults (Holbrook, 1995; Spitz, 1997), which create a generally "D" shaped zone of subsidence (Gagliano et al., 2003). This deformation pattern has been noted in various areas along the Baton Rouge fault, Louisiana (Fig 2.1; Gagliano, 2003a, 2003b). These are distinguishable from other areas of subsidence with less distinct boundaries or random outlines. Prior to the 1970s, neither the Bastian Bay nor the Empire marsh breaks was visible, and the areas of now open water were solid marsh (see Figure 2.2, and Figure 2.3). The Empire marsh break formed between 1976 and 1977. This is according to Greg Linscombe, a biologist for the Louisiana Department of Wildlife and Fisheries

who was flying low transects over the area during this time for purposes of making counts of migratory waterfowl (Gagliano 2002, B.2-1). This general timing is confirmed by a comparison of maps and aerial photos taken in 1971 and again in 1998 (Figure 2.2). The Bastian Bay marsh break appeared around the same time, possibly a few years earlier, and the associated subsidence had drowned the marsh by 1975 (Gagliano, 2003a). This timing was established through eyewitness accounts of local camp owners and checked against aerial imagery.

Here I specifically investigate whether or not there is field evidence of faulting along the linear marsh break which bounds the recently formed water body "No Man's land" located to the west of Empire, Louisiana (Fig. 2.3). Patterns of subsidence and marsh breaks on digital orthophoto quarter quadrangles (DOQQs) and in the LIDAR data are identified as possible markers of active faulting. Cores collected through recent Holocene sediments are correlated to determine whether or not there is any observable displacement across the marsh break. Bathymetric profiles, taken perpendicular to the marsh break across the now submerged area of No Man's Land, help to determine whether the area is deformed by tilting.

Further, if there is a fault, the field data should help to establish whether the fault extends past the observable marsh break. When a segment along a normal fault moves, the largest offset should occur in the middle and decrease as it approaches the segment tips in either direction away from the segment center (e.g., Cowie and Scholz., 1992; Dawers et al., 1993). This general pattern of offset, when applied to the core logs, should also indicate whether the observed marsh break could be interpreted as one large fault segment or many smaller segments. Likewise, the aerial extent of the deformation should

be greatest down dip of the center of the proposed fault segment(s) and decrease towards the tips. This can be applied to both the bathymetric profiles and aerial photographs.

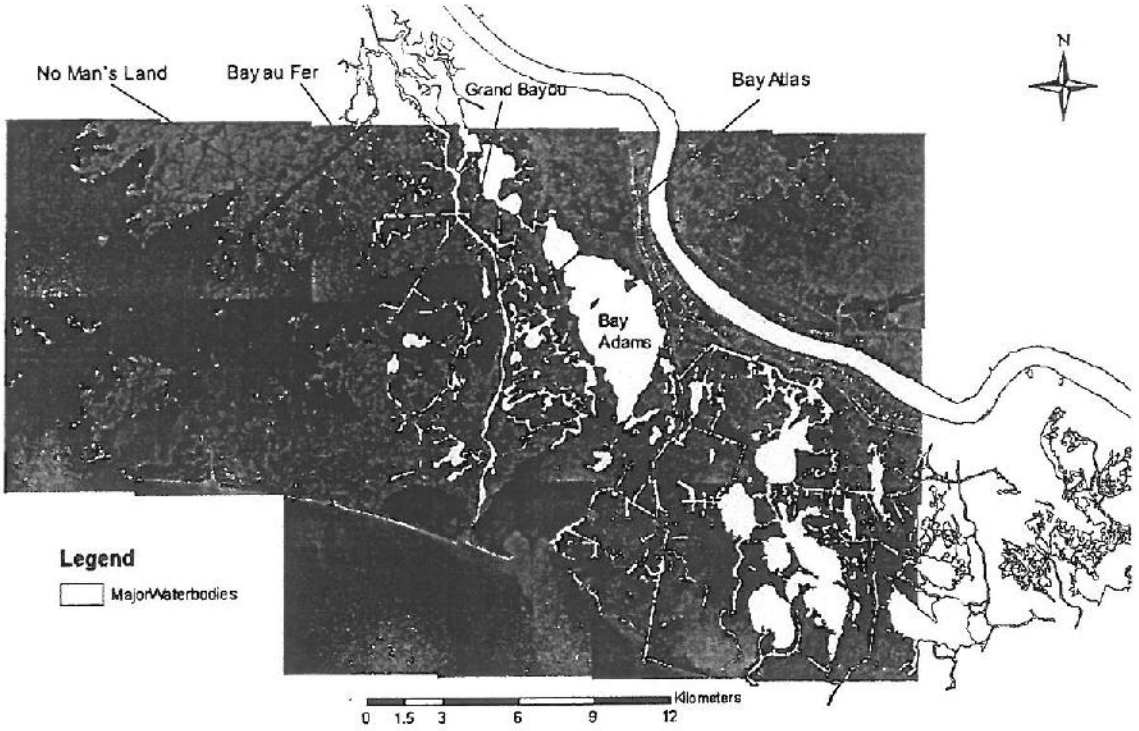

Figure 2.3. Major inland water bodies along the Mississippi (from Penland et. al., 2000) superimposed on USGS DOQQs. Bay Adams and Grand Bayou are among the inland water bodies but the more recently formed No Man's Land, Bay Atlas and Bay au Fer are not.

Methods

The trace of the possible surface expression of the faults in the study area was determined using USGS color infrared digital orthophoto quarter quadrangles, or DOQQs. Fieldwork was done to determine whether the observed marsh break in the Empire area was, indeed, due to faulting. Core transects were taken across the Empire marsh break to identify any offset (Fig 2.4). This included cores both on top of the marsh and in the submerged areas. The cores were taken with a McCauley auger (Fig 2.5); a hand auger that cores at 30 cm intervals. The advantage of the McCauley auger, over other methods such as vibracoring, is that the samples are retrieved without significant compaction; differential compaction can be difficult to distinguish from fault displacement. Cores were described in the field for grain size, Munsell color, organic content, etc. The cores ranged in depth up to 4.3 m, depending on local conditions. A stiff, distinctive clayey zone, containing silt and fine sand layers always dictated the maximum depth (see complete core logs in Appendix 1). Time of coring was recorded and, subsequently, used to correct for tidal variation as measured at the Empire Jetty station.

Samples of organic carbon and peat were obtained where possible. These samples were wrapped in foil, labeled, and stored in a cooler and then refrigerated until they were subsequently dated using Carbon RMS dating techniques. All dating was done by Beta Analytic, Inc. (see Appendix 2). Interpretation of any offsets visible in these transects is based on facies correlation and on the constraints provided by the radiocarbon dates. For correction of radiocarbon dates to calendar dates see appendix A2.

Bathymetric profiles were taken along several transects perpendicular to the Empire marsh breaks. This was done using a manual fathometer with no digital instrumentation. The device was used off the side of a flat-bottomed boat; all data and observations were recorded by hand.

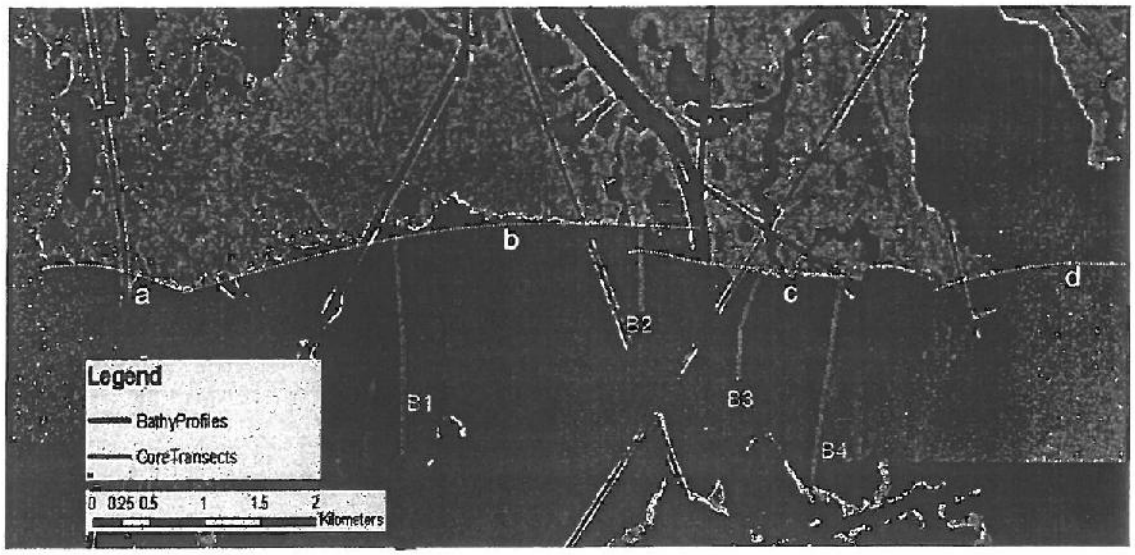

Figure 2.4. The location of McCauley auger transects and bathymetric profiles are shown here along with the proposed location of the fault segments (yellow dashed lines "a", "b", "c", and "d").

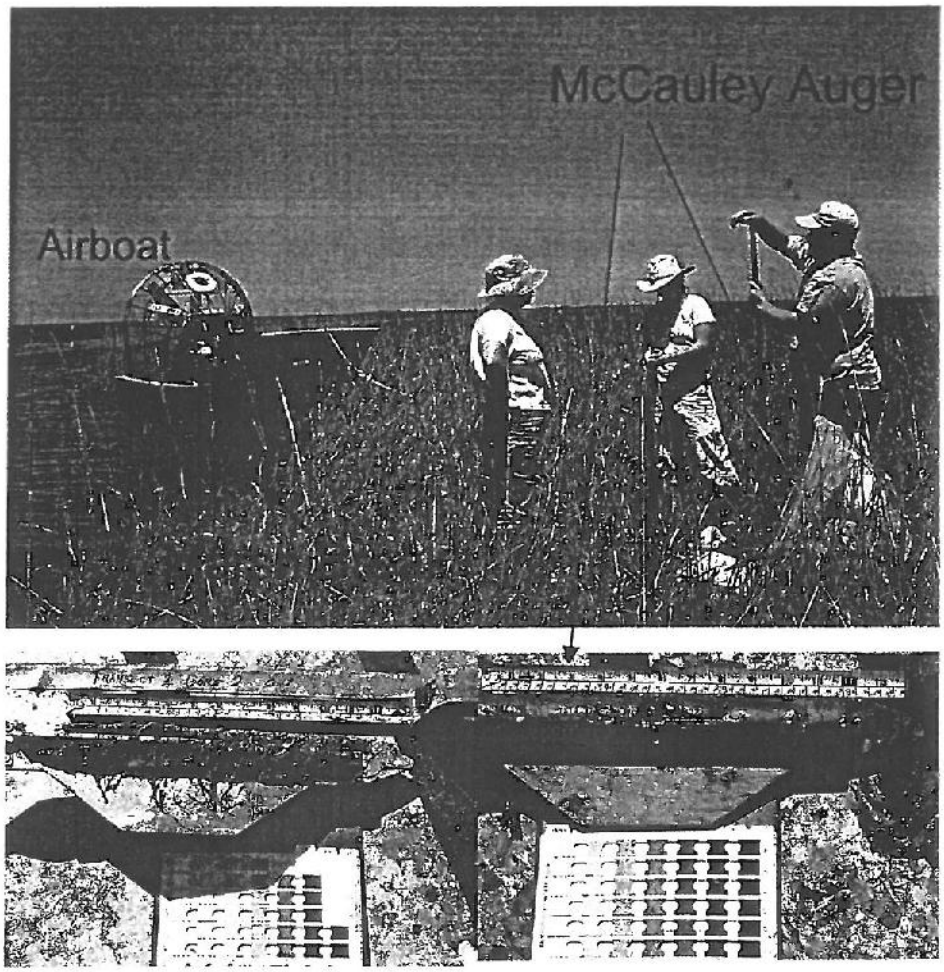

Figure 2.5a. An airboat was employed to gain access to the core sites along the marsh break near Empire. Sections of the McCauley auger are being held by the person at right. **Figure 2.5b.** Close up of a typical sediment core being compared to a Munsell color chart.

Results

Core Data

Figure 2.6 shows the results of all five augered core transects. These transects will be described moving from east (T1) to west (T5). Transect T1 shows a vertical displacement of strata of up to 61 cm. Transect T2 shows little to no offset, except for a very small displacement of sands in the opposite sense. In transect T3 there is displacement in the opposite sense between the first and second cores (C1 and C2). This displacement is correlated using the bottom contact of a well-defined root mat. The correlations between the second and third cores (C2 and C3) in transect T3 show a significant offset both in the physical correlation of the bottom of the root mats and in the difference in age of the two peat samples which were taken at roughly the same depth interval. Transect T4 shows a pattern of offset similar to that seen in transect T3. The correlation in T4 is based on clay layers further down section than the root mats used in T3. The correlation is supported by radiocarbon dates taken at roughly the same depth interval on each of the three cores. Transect T5 shows up to 0.9 m of vertical displacement. This is a larger displacement than that seen on the eastern end of the marsh break in T1.

Radiocarbon Dating

Radiocarbon dates throughout the various cores are consistent with the core correlations based on facies changes (Fig 2.6). Furthermore, they are in the expected age range for deltaic sediments in this area and reinforce the recent time frame of the

observed displacements. The peat samples were all taken from between 0.9 and 3 m below the marsh surface and range from 1520 AD to 970 AD (Figure 2.6). These dates are consistent with more limited dating done previously by Gagliano et al, 2002, (B.3-1) who found dates from a nearby series of vibracores to be within the range of 1340AD-1120AD.

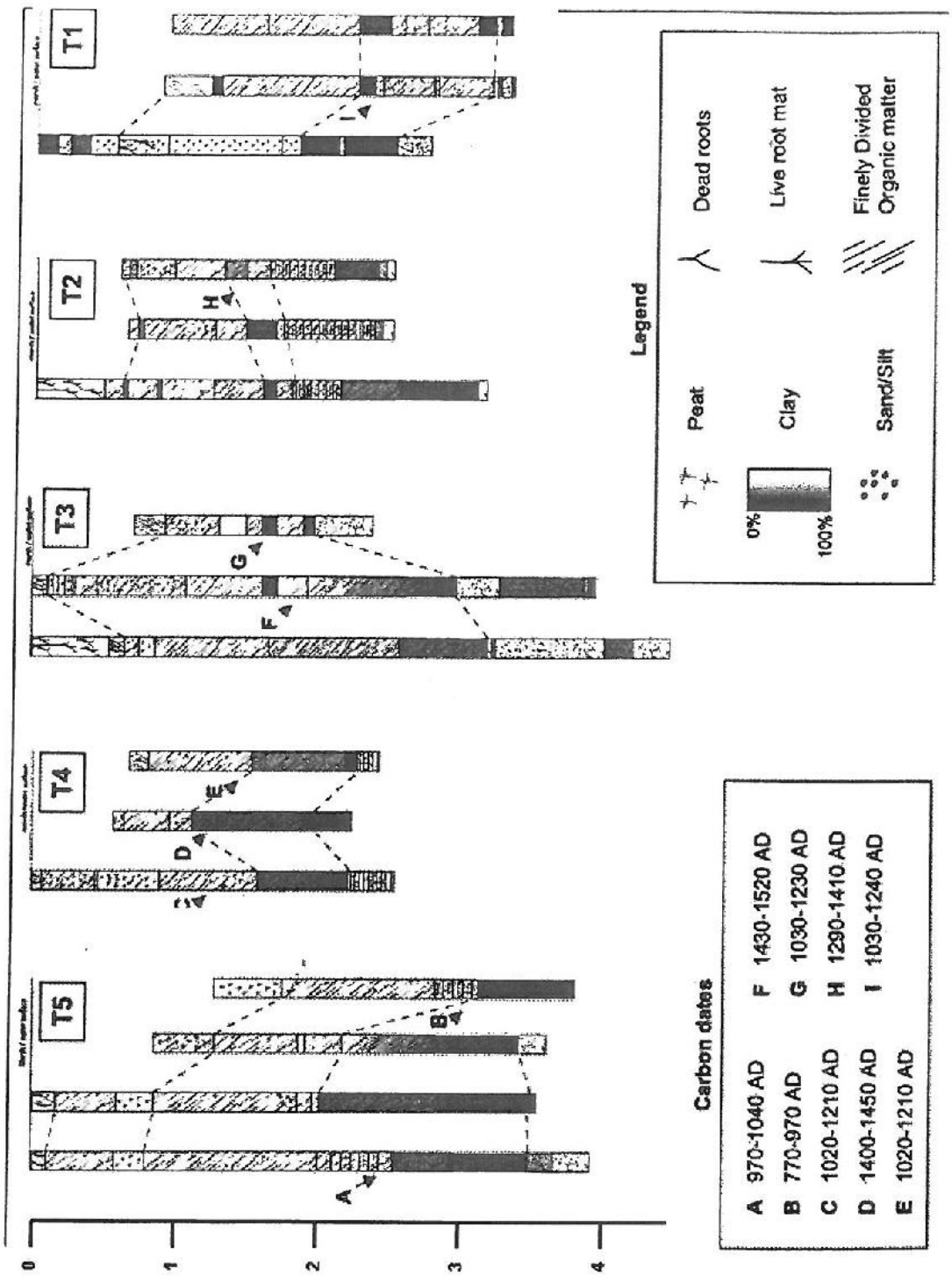

Figure 2.6. Core transects across the Empire marsh break. These are arranged from west (T5) to East (T1). Each transect's cores are arranged from onshore (left) to offshore (right). Datum is local marsh level and is corrected for tidal variations. Vertical scale is tick marked in 1 m intervals. While T1 and T5 show normal displacement, T4 and T3 show displacement consistent with crossing a fault segment stepover zone.

Bathymetric Profiling

Several bathymetric profiles were taken during the 2004 field season in the Empire area perpendicular to the marsh breaks (see Figure 2.4 for location of relevant profiles). With minor variations, all the profiles show an abrupt change in water depth (Figure 2.7). Note in particular that in profile 2 a second bathymetric anomaly exists and correlates spatially with a proposed "step-over" geometry of segments b and c, as discussed below.

The initial abrupt change in Profiles 1 and 2 show almost the same slope and scale. The depth on each is just less than one meter. Similarly, Profiles 3 and 4 show depths of just over one meter. The length of Profiles 1 and 4 allow us to see the gradual shallowing to the south away from the fault structure. This gradual shallowing is suggested in Profiles 2 and 3 as well, as they each show a reduced gradient just before the data cuts off.

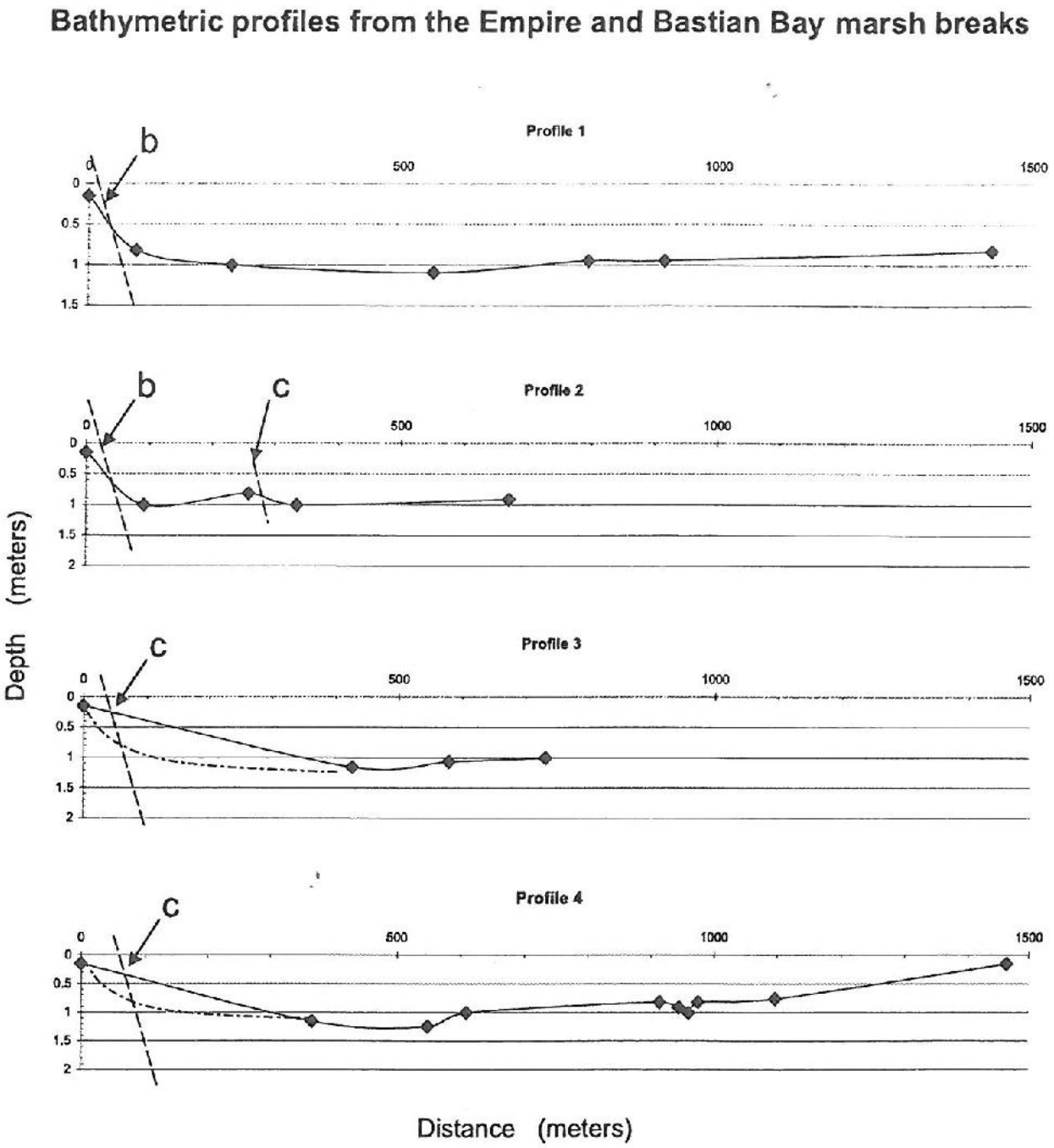

Figure 2.7. Bathymetric profiles south of the marsh breaks at Empire and Bastian Bay. See Figure 2.4 for locations. The diamond shaped points represent where data was recorded. The solid line is the best-fit line. The curved dot-and-dashed lines in profiles 3 and 4 represent possible profiles given the gap in data between the first two points. The short dashed lines show where a given segment (a, b, or c from figure 2.4) of the Empire marsh break intercepts each profile.

Summary and Discussion

The five shallow core transects show a pattern of vertical displacement consistent with the marsh break being controlled by a segmented fault scarp. The variations in offset seen in the cores are consistent with the marsh break being comprised of four fault segments with en echelon overlap. The offsets between facies seen in both T1 and T5 (the eastern and westernmost transects along the marsh break) are consistent with offsets that would be seen if there were a coast parallel, south dipping fault running along the marsh break. The larger displacement seen in the T5 transect could indicate that that transect was taken closer to the center of a segment (interpreted as segment "a" in figure 2.4) than was T1. As T1 is taken very near the eastern most edge of the marsh break, this would indicate that the interpreted segment crossed by T1 (segment "d" in figure 2.4) continues east past the visible marsh break. The lack of offset in transect T2 could be attributed to its placement near the end of an interpreted segment (segment "c"). Displacement should decrease towards the tips of each segment.

The pattern of offset seen in transect T3 and transect T4 is the most compelling evidence for the presence of a segmented fault reaching the surface along the Empire marsh break. Moving from north to south away from the marsh, these transects first show displacement in the opposite sense, followed by normal displacement. This can be explained if the first core in each transect is located on the hanging wall of segment "b" (the western or northern segment). In this interpretation, the second core is then located on top of the footwall of segment "c" (the eastern or southern segment). This would explain the displacement of facies in the opposite sense as they have been down-dropped in the first core and then uplifted in the second. The normal displacement moving from

the second to the third core is then due to crossing fault segment "c". The third core is interpreted as representing the hanging wall of segment "c". The correlations showing these displacement patterns are not only bolstered by the radiocarbon dates but are not easily explained by other means.

The pattern of subsidence seen in the bathymetric profiles is also consistent with a fault scarp producing the marsh break. That is, the abrupt drop at the marsh break and then the more gradual shallowing or "back-tilting" away from the fault comprise a geomorphic pattern that is consistent with a fault controlled landscape and which is seen elsewhere along faults in this region (see Figure 2.1). The interpreted pattern of fault segments "a"-"d" is correspondingly seen in the bathymetric profiles. In profile 2 there is a second anomaly at the point along the profile where segment "c" is interpreted to intercept the profile (Fig 2.7).

Since any original scarp-created marsh break would surely have been somewhat altered by wave action and edge erosion in the years since it had formed, the current marsh break should not be interpreted as precisely representative of the shape and location of any original scarp. However, the general shape of the marsh break still clearly suggests fault segments. Furthermore, the pattern of the facies contacts across the marsh break are still telling and correlate with activity parallel to and in the immediate vicinity of the marsh break. These correlations are not invalidated if the break has been superficially changed or eroded back even a few meters. In fact, some of the strongest surface evidence for fault-induced subsidence is the shape of the bathymetric profiles as they move away from the marsh break. This gradual shallowing (or diminishing of the

3D displacement field) away from the marsh break (where recent displacement is greatest) is not expected to be affected by any localized erosion of the marsh break itself.

The above results suggest faulting took place post ca.770 to 970 AD, indicating that the marsh break west of Empire represents a Holocene fault scarp. Moreover, because the displacement documented by the correlation of the cores does not die out at the east and west ends of the sampled area, if this is a fault, it is likely longer than the observable marsh break in both directions.

Land loss through subsidence is a problem throughout coastal Louisiana. The causes are many and complex. Initial subsidence can be caused by multiple factors and then subsequent edge erosion on newly exposed marsh breaks exacerbates the problem (Wilson and Allison, 2006). Faulting is not always the leading cause. Just to the east of this study area in Barataria Bay, Louisiana, there have also been high rates of marsh loss due to subsidence and subsequent wave action. There the subsidence is most likely due to varying amounts of compaction within the underlying geology. Unlike Empire, the geometry of the marsh breaks in Barataria is not consistent with surface faulting, additionally, core transects taken there do not show a pattern of offset indicative of faulting (Wilson and Allison, 2006). In that area, the subsidence (measured from the base of a peat layer) increases with increasing distance from marsh break out past 400 meters. In contrast, the measured offset in the Empire cores is abrupt across the marsh break (see Transect 1 in Figure 2.6). A true comparison, however, of core data from the two sites would need cores taken at more similar intervals for each site.

The fact that comparable areas nearby have experienced similar losses, ostensibly without faulting, is motivation to deepen our inquiry into the structure of the Empire and

Bastian Bay areas. The surface data here, unlike surface data in some of the surrounding areas, possibly indicates active faulting. While this surface data is not unequivocal, it does correlate in every respect with the initial interpretation of faulting and with the pattern of fault segments hypothesized from the pattern of marsh break seen in the DOQQs. In the sections below (Chapter 3), the subsurface of the study area is explored to (1) confirm the existence of faults and (2) to determine, if present, whether they are small and localized or regional in extent.

CHAPTER 3: STRUCTURE AND KINEMATICS OF FAULTS NEAR EMPIRE AND BASTIAN BAY, LOUISIANA BASED ON SUBSURFACE DATA

Introduction

The surface data presented in Chapter 2 indicate that the marsh breaks at Empire and Bastian Bay are consistent with fault scarps and that the fault itself likely extends to the east and to the west of the visible breaks. Here subsurface data is used to determine if any such faults exist below the marsh breaks. Subsurface faults correlating to the surface marsh breaks are identified, named, and related to previously mapped faults (Meltzer, 1966; Sabate, 1968), and further, their size and structure is investigated. Their size and structure should help clarify whether the identified subsurface faults ("Empire fault" and "Bastian Bay fault") are en echelon fault segments of a larger system or two separate fault systems. In addition, information on the timing of past fault displacement can also be determined from the subsurface data. Three types of subsurface data are used in this study -- paper well logs, proprietary paper seismic lines, and digital seismic lines from an offshore proprietary grid located further to the east.

Well Logs

The most abundant and readily accessible source of subsurface data in the Empire and Bastian Bay areas are well logs. An extensive collection is maintained by the State of Louisiana's Department of Natural resources (DNR) in Baton Rouge. Although seismic reflection data acquired by the hydrocarbon industry offers obvious advantages over well

log data for unequivocally identifying faults, the non-proprietary nature of the well logs makes them the most useful information source for this study.

***Well Log Methods*:**

Publicly available paper well logs were obtained from the Louisiana Department of Natural Resources (DNR; Figure 3.1). These are very large format plots that are too large to be easily interpreted using common software. All interpretation was done by hand using hand-traced copies of analogue resistivity and spontaneous potential (SP) curves (Figure 3.2). For complete correlations see Appendix A3. Standard subsurface geologic mapping correlation techniques were used (see Tearpock and Bischke, 2003). Appropriate wells were picked ranging from north of the Empire marsh break to south of the Bastian Bay marsh break (see Figure 3.1). The logs were chosen based on their location in relation to the observable surface features, discussed in Chapter 2, and also based on their depths. In order to relate subsurface features to surface features, logs with data at the shallow depths were preferentially chosen. After the wells were correlated, the horizon data was then projected into a north-south cross section (see results).

Resistivity is a measure of how resistive a formation is to the flow of electricity. Saltwater has very low resistivity and oil and gas reservoirs have very high resistivity. Spontaneous potential (SP) is a measure of the natural electrical potential of a formation. SP curves help determine the permeability and salinity of various beds. SP profiles are generally more negative for sands and more positive for shales. Resistivity should be less variable for shales and, for sands, should show more extreme variations toward lower resistivity if the pore space is filled with salt water or toward higher resistivity for a

hydrocarbon reservoir. Using both of these curves (where available) gives a good measure of confidence in the validity of the interpretations. The depth intervals over which the correlations were made is somewhat dependent on well log availability. In all cases the correlation was begun at the shallowest possible depth. In six of the wells the correlation began between 100 m and 150 m. In most cases, the correlation was extended to depths >2500 m (see Figure 3.3).

Expansion indices (EIs) were calculated for the two major faults in question: Bastian Bay fault and Empire fault. To derive expansion indices, the ratio of hanging-wall to footwall thickness for each stratigraphic unit displaced by the fault is calculated (Thorsen, 1963). This shows intervals during which stratigraphic "growth" has taken place; i.e., a thickening in hanging wall depocenters marking a time interval when the fault was actively accruing displacement. Figure 3.4 illustrates how expansion indices are calculated. For this study, the indices were calculated using the data available from the correlation of the well logs.

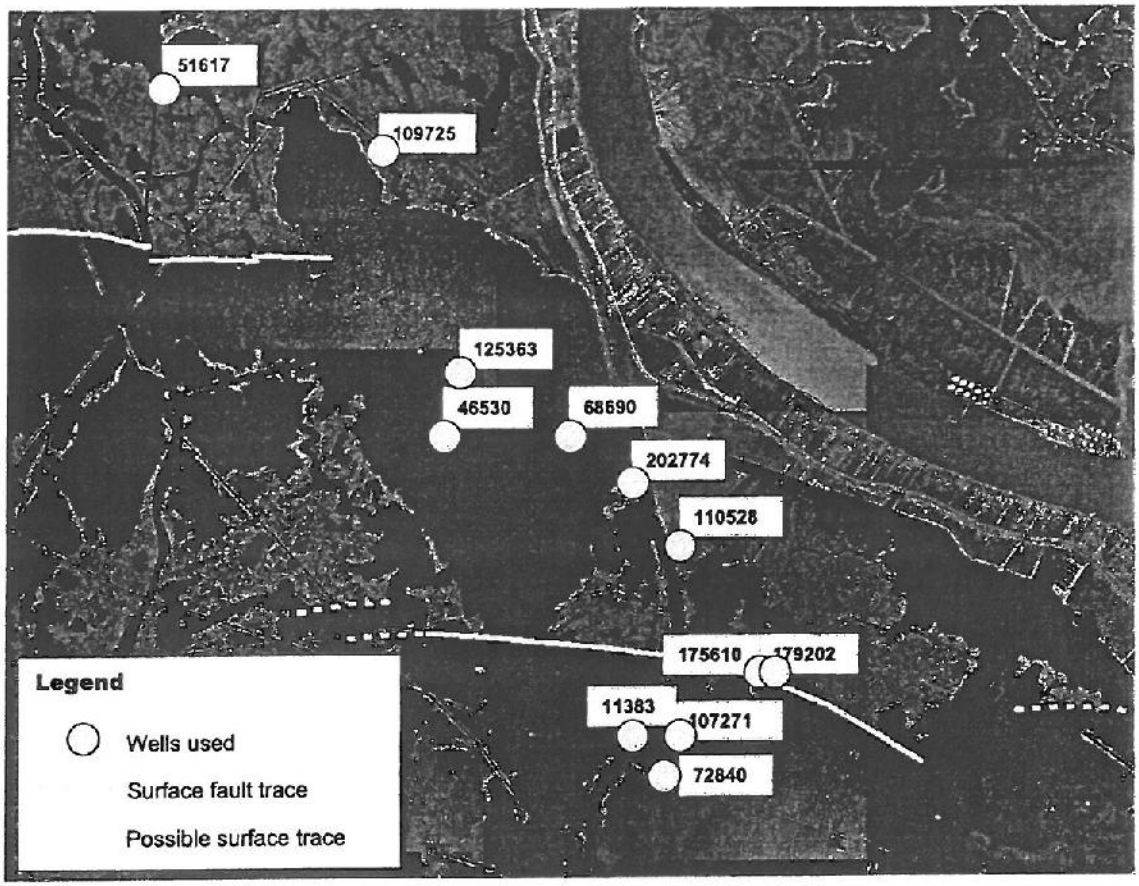

Figure 3.1. Locations of the various well logs used in the vicinity of the Empire and Bastian Bay fault segments.

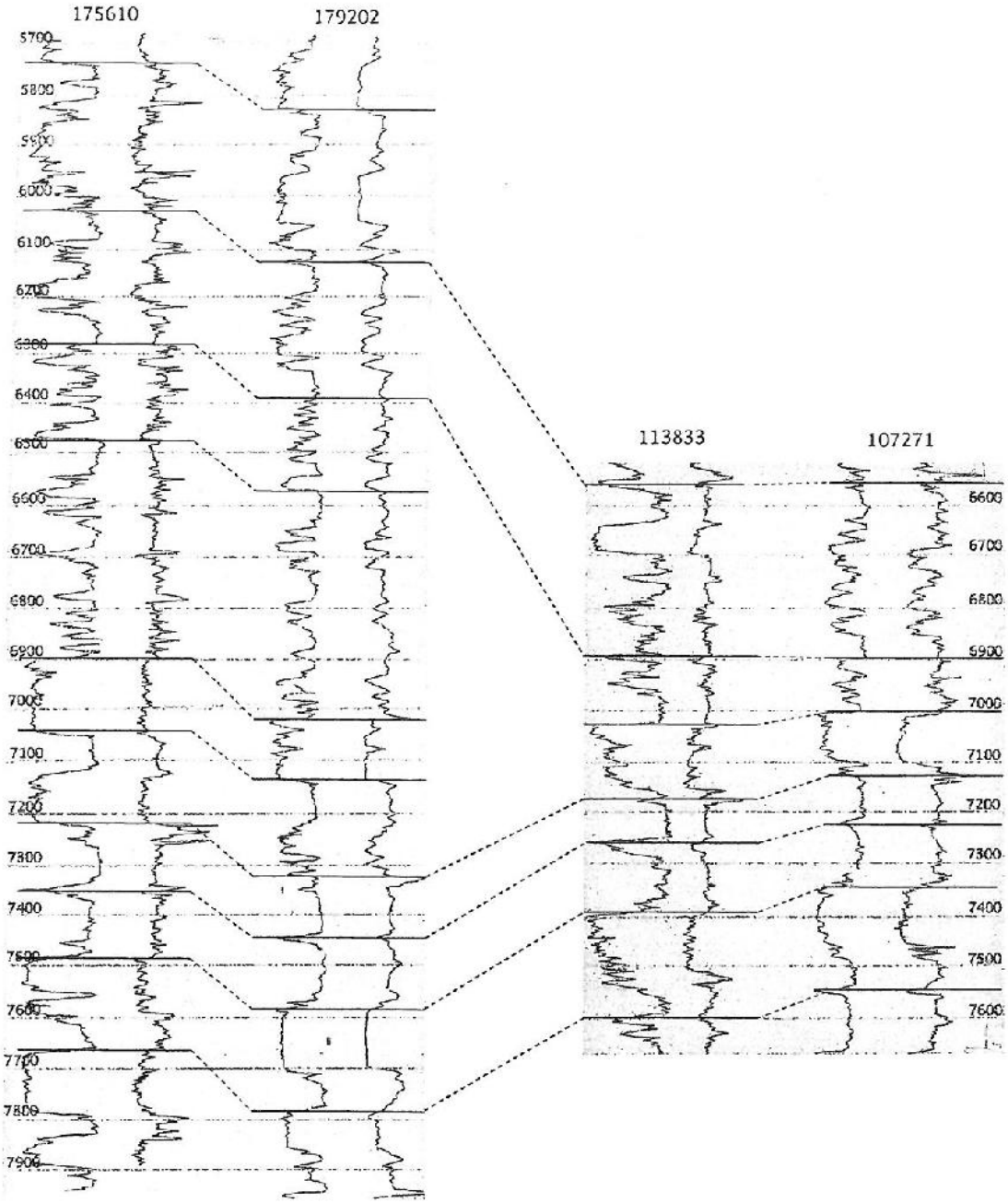

Figure 3.2. Sections from four well logs with interpretation are shown as an example of how the work was done. The depths are in feet as on the original well logs. Depths were later converted to meters. The curve at left for each of these logs is the resistivity; the right curve is the SP. Missing sections in 11383 and 107271 are interpreted as indicating a fault cut.

Well Log Results

Data from the wells shown in Figure 3.1 were projected onto a cross-section oriented north-south, roughly perpendicular to both the Bastian Bay and Empire marsh breaks. The interpreted cross-section identifies and traverses both the upthrown and downthrown blocks of two large faults that correlate to the two marsh breaks. In response to this correlation these two faults were named the "Empire fault" and the "Bastian Bay fault" and are hereafter referred to as such (Fig 3.3).

Numerous smaller faults can be seen deeper in the section both north of the Empire fault and between the Empire and the Bastian Bay faults; however, none of these secondary faults show any evidence of reaching the surface. Both large faults, on the other hand, do indicate displacement in the shallow part of the stratigraphy.

Neither of the larger faults shows consistent "growth" or thickening of the stratigraphy on the down dropped side, but instead show distinct sections of stratigraphic growth interrupted by sections with offset but no growth. As stratigraphic growth is the direct result of fault activity, the analysis shows a kinematic history of intermittent activity. On the Bastian Bay fault, small variations in movement are such that no consistent pattern in offset and growth are visible at smaller scales. Grouping strata into larger packets shows an episodic pattern of expansion of the downthrown packets across the fault. Packets showing no significant expansion or growth interrupt these expanded packets. The expansion indices are significant in two places: one at depths roughly between 1600 and 2000 meters and again in the uppermost 700 meters of the stratigraphy (Figure 3.5). Between these two intervals there is still significant fault displacement without growth. This indicates that the fault was active early in it overall displacement

history, as evidenced by growth in the deeper section, and again more recently recorded by growth in shallower section. During this recent period, offset occurred over a large portion of the existing fault resulting in offset with no accompanying growth in middle section. The pattern for the Empire fault is similar to that of Bastian Bay, although expansion is present in shallower sections. The two periods of significant stratigraphic expansion are between 0 and 200 meters and between roughly 1100 and 1600 meters.

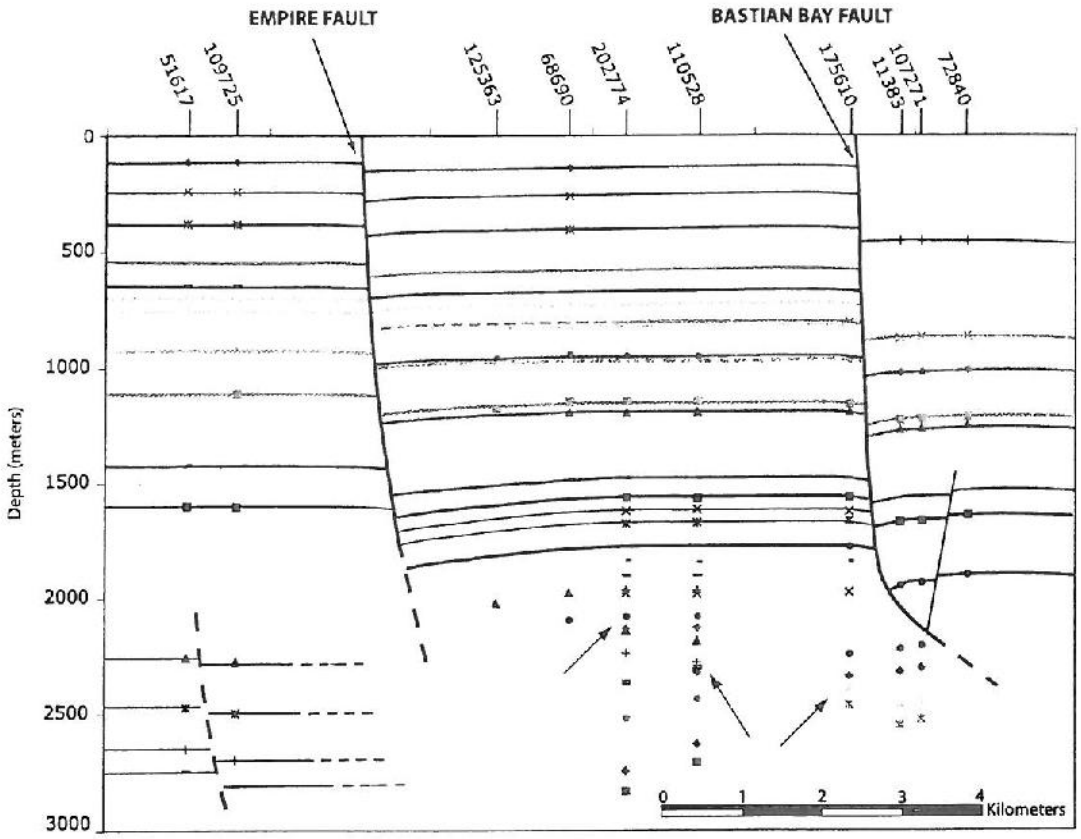

Figure 3.3. The Empire and Bastian Bay Faults are interpreted here using the well log data. Each marked point represents a point of correlation. Several deeper, unmapped, faults are indicated by offset horizons and missing sections (indicated by grey arrows).

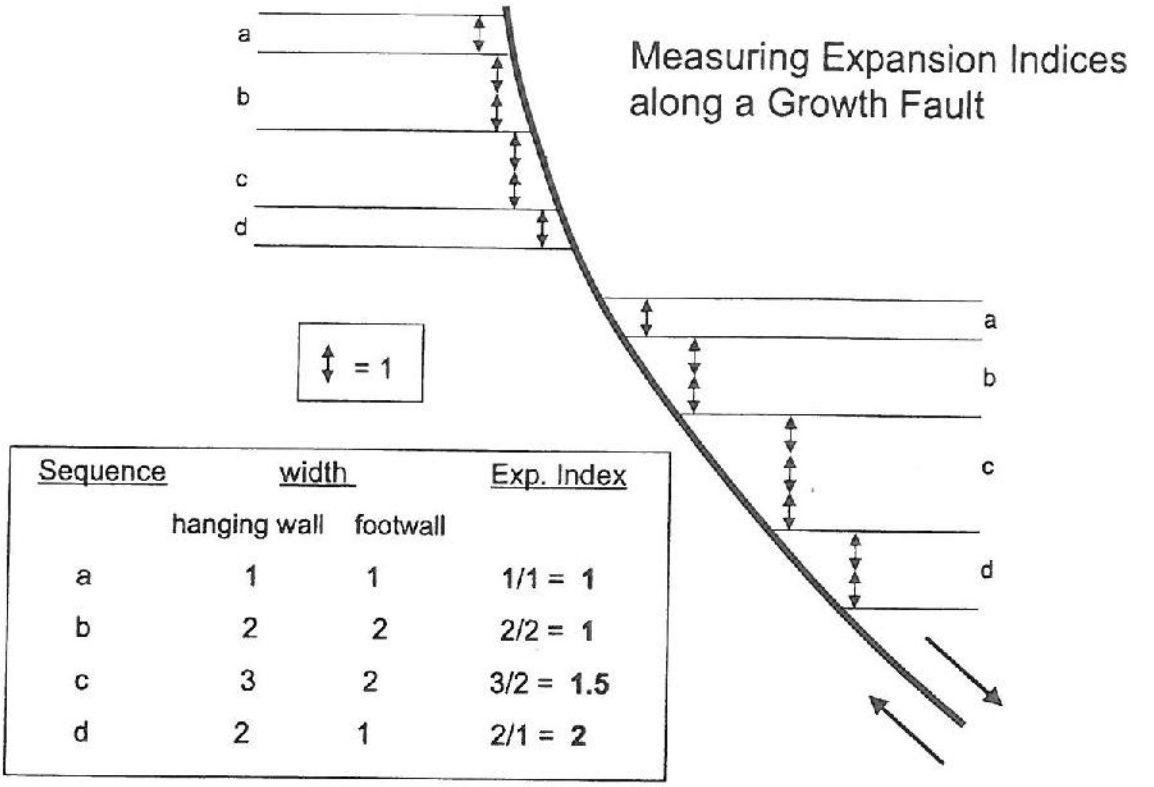

Sequence	width		Exp. Index
	hanging wall	footwall	
a	1	1	1/1 = **1**
b	2	2	2/2 = **1**
c	3	2	3/2 = **1.5**
d	2	1	2/1 = **2**

Figure 3.4. An example of how expansion indices are measured. Divide the thickness of the downthrown layer by the thickness of the corresponding upthrown layer. An index of 1.0 means that fault displacement occurred after the deposition of that interval, rather than during it.

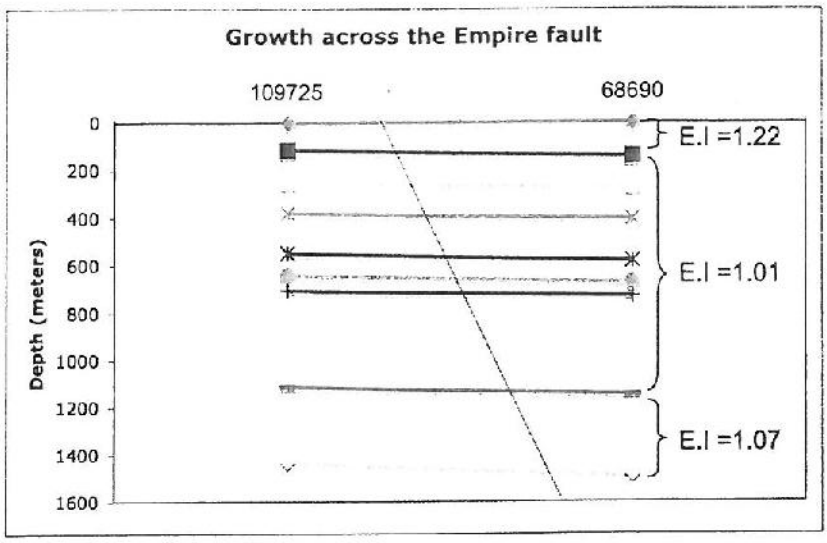

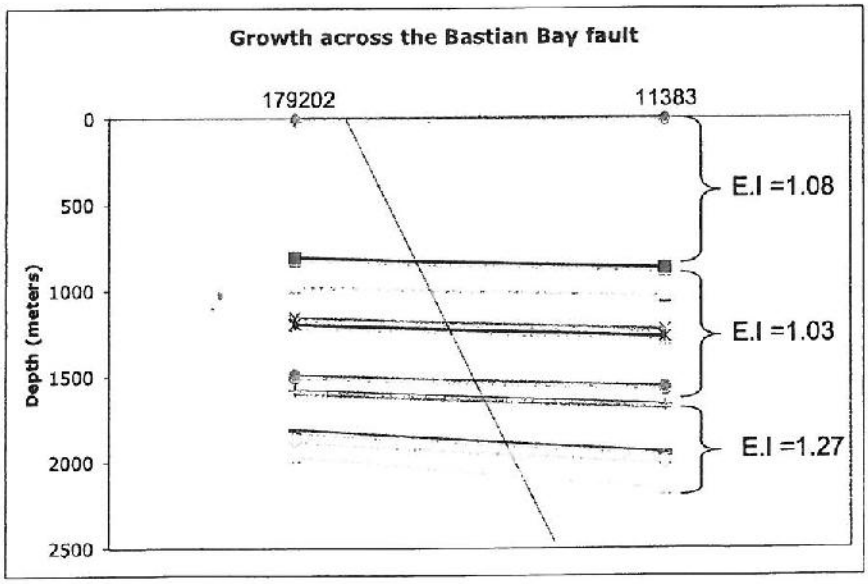

Figure 3.5. Data from four wells, one on the upthrown and one on the downthrown block of each fault, demonstrates the relative stratigraphic expansion, or "growth" across the faults at different intervals. An expansion index EI = 1 indicates no expansion, EI > 1 indicates some growth, or in other words, a time interval of active faulting. The dotted lines serve as reminders of the fault location.

Well Log Discussion & Summary

Lack of consistent stratigraphic growth suggests that a portion of the activity along both the Empire and the Bastian Bay faults is geologically youthful and may post date much of the sediment accumulation here. The two distinct periods of growth shown on the Bastian Bay fault suggest a period of fault activity in the Miocene and then again more recently, sometime in the Pleistocene or Holocene. Sabate (1968) mapped the basal Pleistocene in the Empire and Bastian Bay area between 600 and 760 meters depth. As the more recent period of growth in Bastian Bay is somewhere between 700 meters and the surface, this movement occurred no earlier than the Pleistocene.

To narrow down the time frame of the more recent movement, more detailed data is needed in the hanging wall section of the Bastian Bay fault between 0 and 700 meters. The total displacements during these two active periods are comparable, but the expansion indices, although observable in both, are higher in the Miocene section. This suggests that the more recent activity is either very recent and so the accumulation of sediments has not reached its peak, or that, whatever the precise timing of the more recent activity, there was movement on the fault without significant influx of new sediment. There has either not been time or material for accumulation on the scale of the Miocene movement at the Bastian Bay fault.

As pointed out in the results section above, the Empire fault shows a similar growth pattern to the Bastian Bay fault, but with shallower data the more recent era of activity can be narrowed down to somewhere in the upper 200 meters of sediment. This probably corresponds to late Pleistocene, as the base of the Holocene is somewhere between 70 and 110 meters (Meckel et.al., 2006; Kulp et.al., 2002). Both the shallow

core transects taken at the eastern edge of the Empire marsh break (see Chapter 2) and the well-expressed offset observed in the well log-cross section that is located just east of the end of the Empire marsh break, suggest that the Empire fault extends east of the marsh break. More data is needed to determine the eastern extent of the fault. While the cores suggest that one particular interpreted segment extends east, it is not known how far or whether that same segment would be large enough to be responsible for the deeper offset observed in the well logs. There may be yet another en echelon segment to the east of the marsh break (Fig 3.6). If the Empire fault does extend east of the marsh break, it is unlikely that the Empire and the Bastian Bay faults represent two en echelon segments of a larger system, as it is uncommon for that much overlap to be found on two interacting segments (e.g., Gupta and Scholz, 2000).

The surface cores discussed in Chapter 2 extend, at most, 4.3 meters below the surface and the shallowest well logs begin at 60 meters. This gap in the data will need to be addressed in future studies, perhaps with shallow seismic surveying of the Empire area. For purposes of this study, the fault surface, as interpreted from the subsurface data, will be projected up to its likely termination at the surface and then this projection compared with the observed surface features.

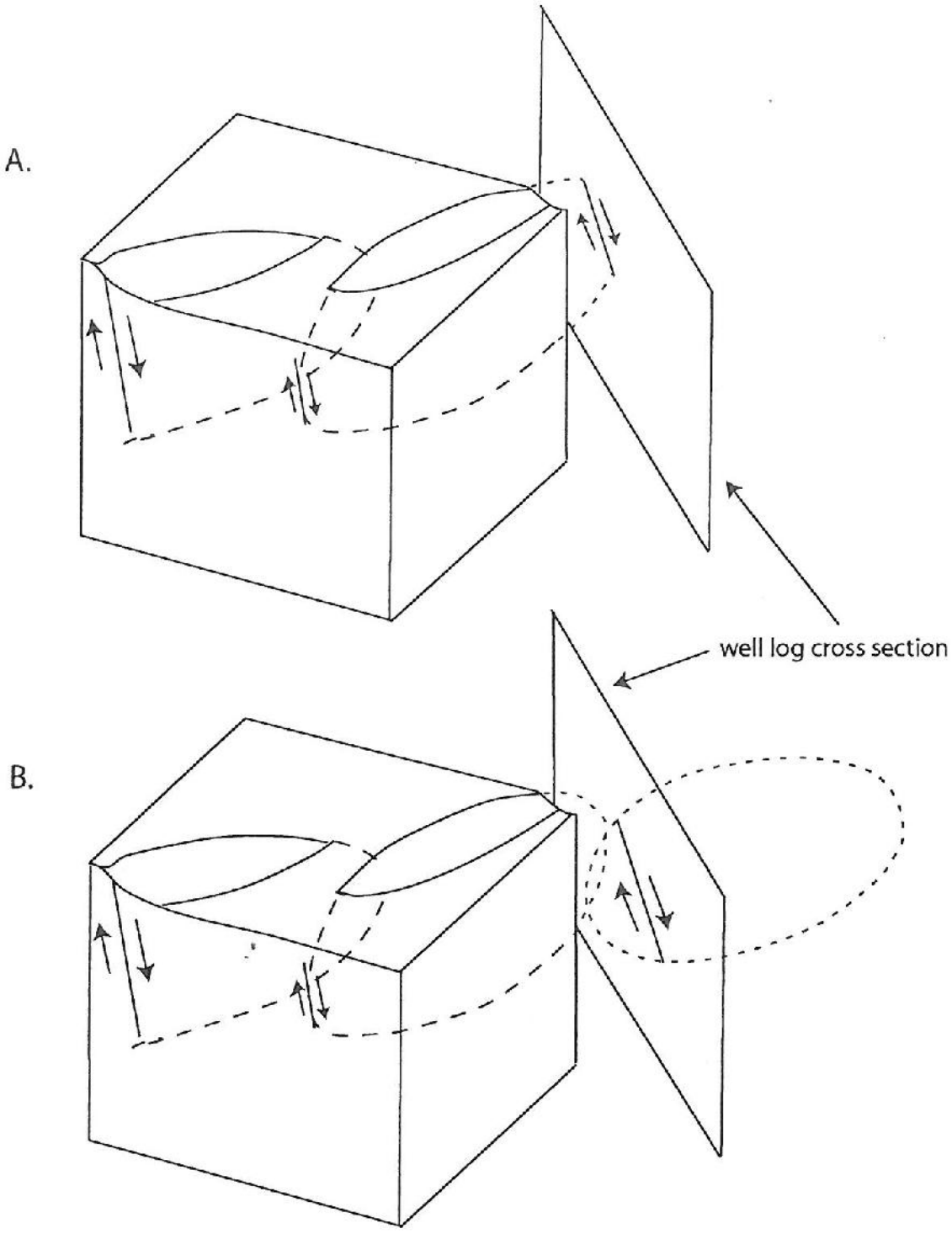

Figure 3.6. This schematic of the Empire fault represents the segments of the fault proposed to be visible as the marsh break at the surface, and then shows two possibilities for displacement observed further east. Either the last visible segment extends eastward or there is another segment in the system.

Onshore Seismic data: Empire and Bastian Bay

Seismic data is a very useful because it can provide a more detailed visual picture than well logs along a given two-dimensional section. Unfortunately, there have been fewer seismic lines shot in the immediate study area than in some of the surrounding areas. Moreover, the proprietary natures of the lines that do exist make them difficult to obtain. Nevertheless, a few relevant and interpretable lines were obtained for this project.

Onshore Seismic Method

Proprietary paper seismic lines from Seismic Exchange, Inc. were used to confirm the findings from the well log data. The seismic lines also give a more precise location of the faults indicated by the offsets in the log cross-section. Interpretation of the paper seismic was done by hand with the aid of "cut and paste" techniques to match up horizons on the footwall to their corresponding other halves on the hanging wall. As the top few tenths of a second (two-way travel time, TWTT) of seismic data are distorted, the faults that are continuous through the shallow part of the data were projected to the surface following their basic geometry, i.e. assuming a constant dip in the near-surface, and then marked on a surface map using the shotpoint data (Fig 3.7).

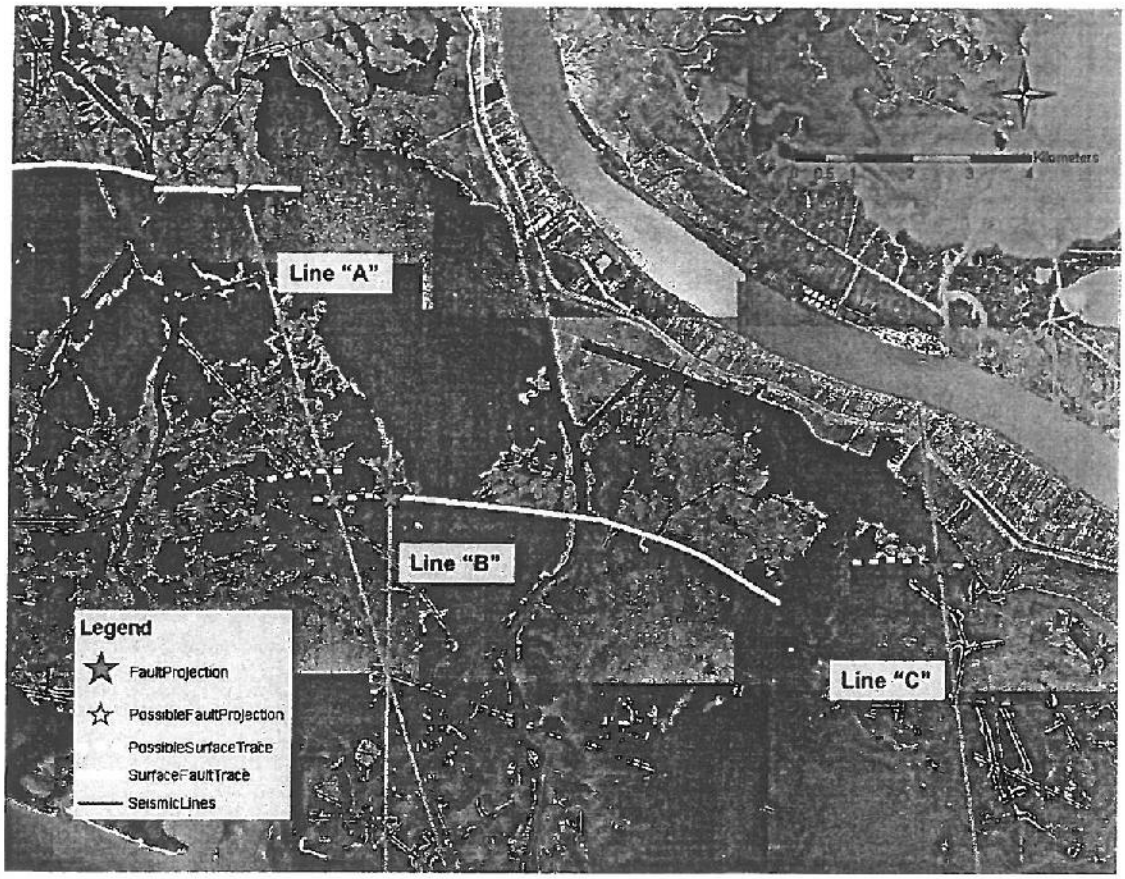

Figure 3.7. Projection of the subsurface faults from the paper seismic data shows them reaching the surface at the Bastian Bay marsh breaks. The Empire fault projection is an estimate, as the seismic line cuts off before the fault can be followed to the near surface.

Onshore Seismic Results

Three seismic lines with sufficiently clear reflections were located in the Empire and Bastian Bay fault zone. These are here referred to as lines "A", "B", and "C" (see Figure 3.7 for locations). Interpretation of these lines show major, slightly listric, faults striking roughly coast parallel, corresponding spatially with the surface features (marsh breaks at empire and Bastain Bay) and with the well log data (Figures 3.8, 3.9, and 3.10).

Clear offset is observed across the Bastian Bay fault in Line "A"; this displacement includes the uppermost clearly defined reflections (Figure 3.8). This is a large fault along which displacement increases with depth, implying a long history of movement. The smaller fault south of the Bastian Bay fault has accumulated less offset and does not appear to reach shallow portion of the seismic data. This fault may have died out with subsequent displacement accumulating solely on the nearby Bastian Bay fault. Alternately, the earliest movement may have been on the Bastian Bay fault, and, then, as it aged, the smaller fault may have formed to the south (outboard) of the initial plane of the Bastian Bay fault. The smaller fault may represent a new incarnation of the first Bastian Bay fault. This offshore migration in the locus of faulting is common in growth faults. They will stereotypically migrate offshore, growing, rotating and then, at some angle, dying out, after which, a new segment will propagate just basinward of the original (Mauduit et al., 1998). During a more recent period of reactivation, the older Bastian Bay fault may have been the preferred plane of movement, with the smaller outboard fault remaining less active. The latter interpretation may be preferable, as the outboard fault continues to show offset through the period where no clear offset is

observed in the Bastian Bay fault, i.e., at about 1.2-1.7 seconds TWTT (see Figure 3.8). This could represent a period of time during which the Bastian Bay fault temporarily stopped moving, and through this period deformation was accommodated by strain on the outboard fault. There is at least one small antithetic, i.e., north dipping, fault shown here as well. This is common in all normal fault systems.

The northernmost fault projects roughly up to the surface along the Empire marsh break and may, indeed, be the Empire fault, however, without better shallow data it cannot be confirmed. Line "B" shows the same two Bastian Bay faults, but the uppermost portion of the seismic line is clear (Figure 3.9). This line confirms the interpretations of line "A", with the same strong reflectors showing similar offset patterns.

Note that both of these lines cross the Bastian Bay fault at the westernmost edge of the visible marsh break, here attributed to Holocene displacement on the Bastian Bay fault. Because there is significant total throw (vertical displacement) along the faults, almost .5 seconds TWTT, it may be inferred that the Bastian Bay fault ends some distance west of the edge of the marsh break discussed previously. Overall, there is compelling evidence for multiple periods of activity, as the large faults have discontinuous growth and offset that may indicate periods of quiescence. Thus, along what looks like, at low resolution, a large continuously dipping cross section of a fault, in detail shows areas with no resolvable displacement. This is illustrated in Figure 3.8 by the dashed lane and question mark along a portion of the Bastian Bay fault.

Line "C" shows a large south dipping fault that projects upward to the surface at the eastern end of the Bastian Bay marsh break (Figure 3.10). The upper reflections in the line are not clear enough to follow the fault trace up to the surface with confidence, but

offset can be observed in the uppermost clear reflectors in the seismic line. There is also an antithetic fault that is cut by another, but more recent, small antithetic fault. This is a similar pattern to one mapped to the east of the study area in Sabate's (1968) work (discussed below). The main south-dipping fault here is listric and clearly extends down into the section to roughly 3 seconds TWTT.

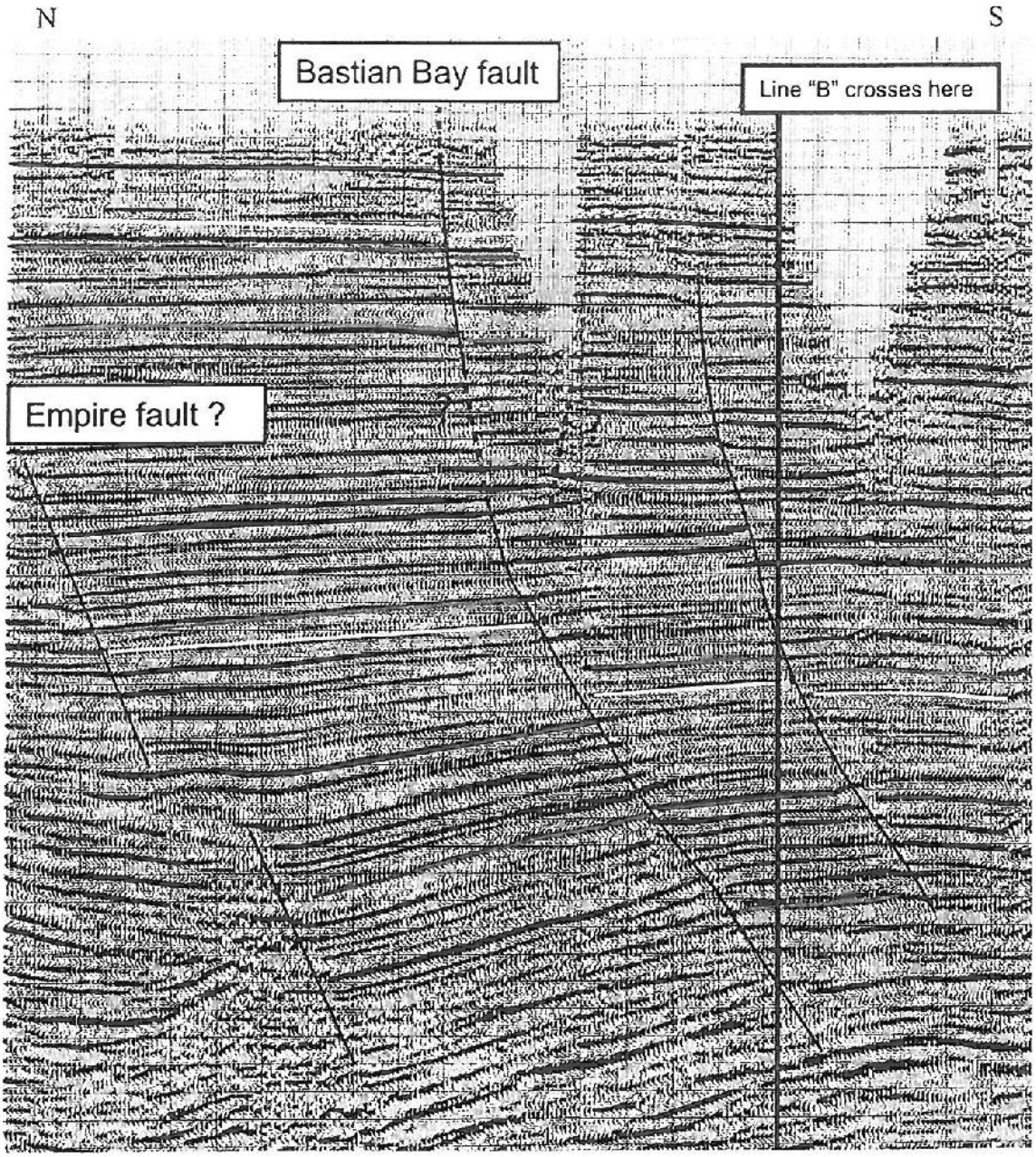

Figure 3.8. Line "A". This line clearly shows a fault extending upward towards the Bastian Bay marsh break at the surface, with visible displacement of the shallowest discernible layers. While displacement is clear in the lower and upper portions of the Bastian Bay fault, there is an ambiguous area between 1.2 and 1.7 seconds where displacement, if any, is unclear. The fault indicated at the northern edge of the line may possibly be the Empire fault.

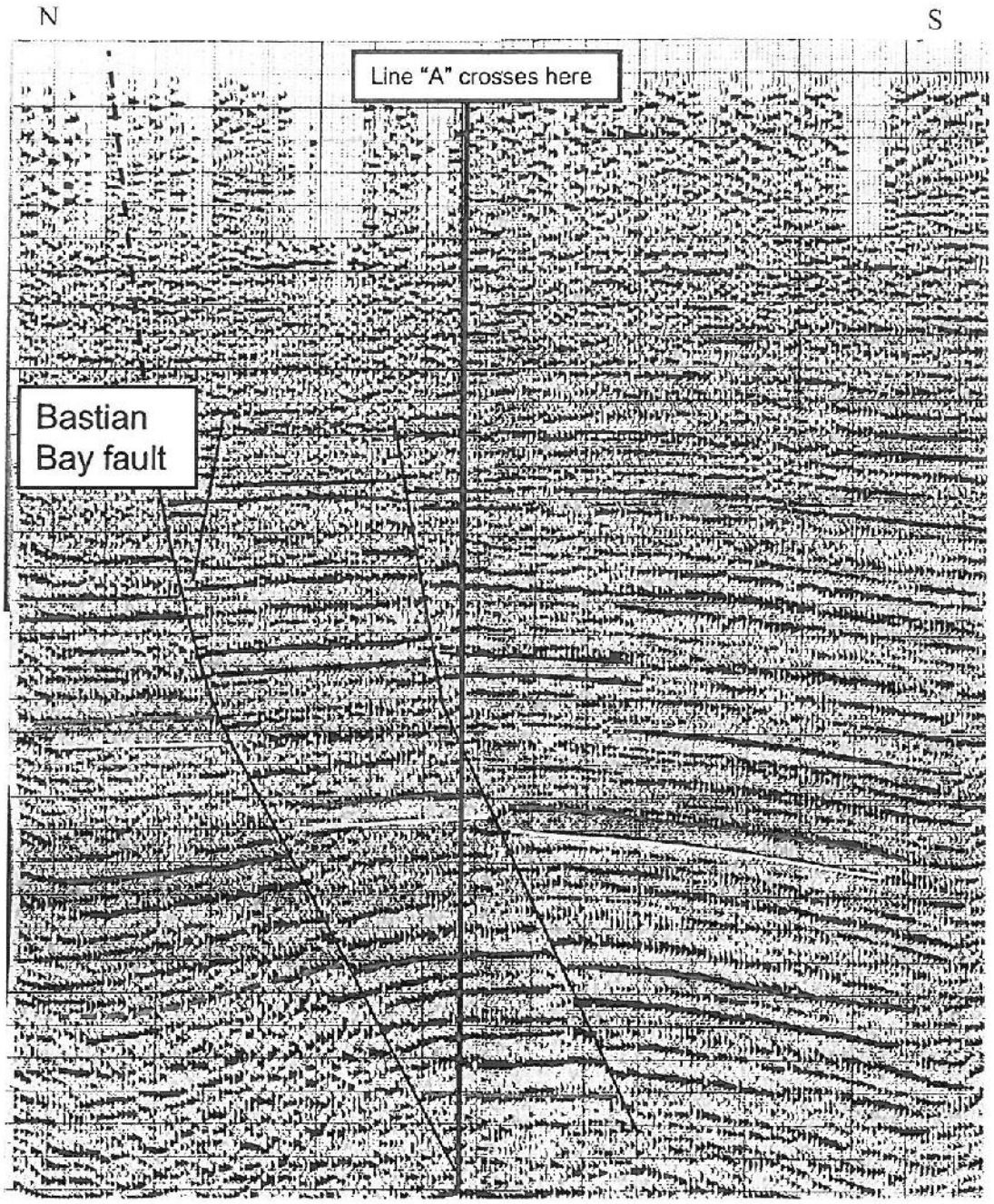

Figure 3.9. Line "B". This line shows much the same information as in the previous figure, although it does not extend as far north and therefore does not capture the surface trace of the Empire fault. The shallow data is not clear and so the continuation of the Bastian bay fault to the surface is shown by a dotted line. The horizons here have the same colors as their counterparts in Figure 3.8 above.

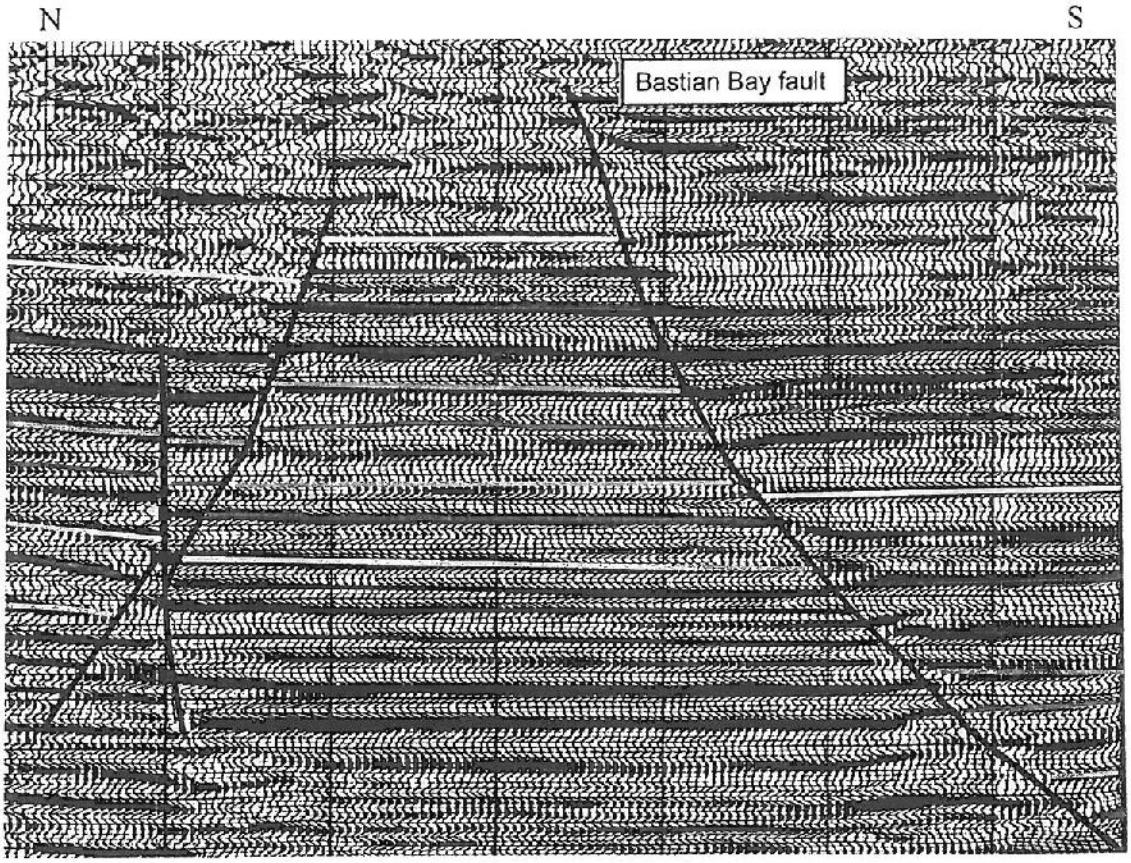

Figure 3.10. Line "C" is to the east of the previous two lines (see Figure 3.7 for location). This shows the Bastian Bay fault with a displacement of approximately 0.55 seconds TWTT. The north-dipping fault has less displacement (approximately 0.1 second TWTT) and is intersected by a small antithetic, south dipping fault that is younger than the fault it cuts.

Onshore Seismic Discussion and Summary

An approximated displacement profile, constructed using the three points where these seismic lines cross the Bastian Bay fault, shows an intriguing pattern (Figure 3.11). Using strongly reflective horizons located around 1.7 seconds depth in the footwall, the displacement was measured for each line. The displacement increased by a significant amount to the east from 0.150 seconds to 0.625 seconds TWTT. As displacement increases towards the center of a fault or fault segment, an increase indicates that the fault is not dying out but continues. This implies that the fault continues well to the east which would have it crossing the Mississippi River. To determine whether this trend is significant, more industry seismic data needs to be examined to fill in the gap between the two lines to the west and the one to the east.

The available data indicates that there is a large, south dipping, normal fault with peak displacement near the river, which has been shown to be active during the geological recent past. Displacement profiles discussed below from mapping done by Meltzer (1966) in the Bastian Bay area are more detailed and show large displacement towards the west end of the data. While the data obtained from the well logs and from the paper seismic data seems to corroborate one-another, a more thorough analysis involving accurate depth conversion of the seismic data is needed. The data needed to construct accurate velocity profiles in this area is unavailable at this time.

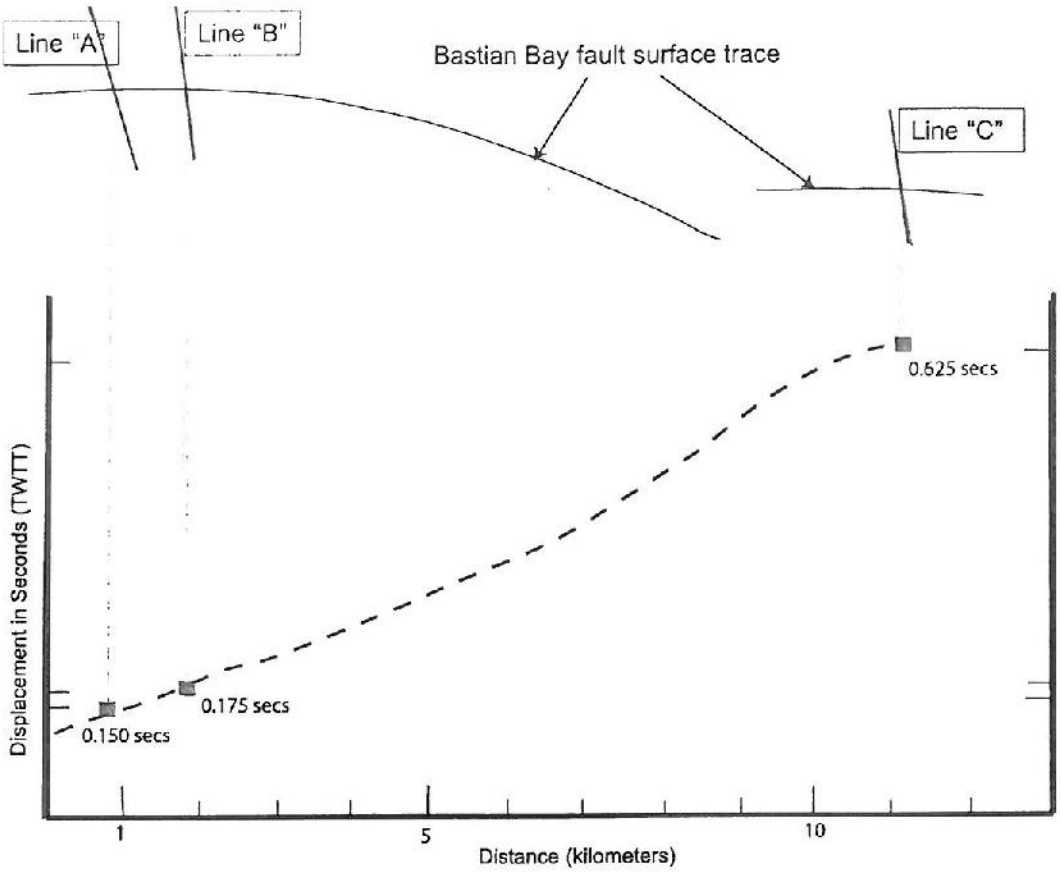

Figure 3.11. Displacement profile along the visible segments of the Bastian Bay fault at a depth corresponding to roughly 1.7 seconds TWTT. Displacement was measured from the three seismic sections discussed here.

Displacement Profiles from Previous Work

Displacement profiles have been shown to have a characteristic tapered shape with greatest displacement near the fault center (e.g., Cowie and Scholz, 1992; Dawers et al., 1993). Skewed profiles generally indicate interaction with nearby fault segments whose movements define areas of relative accumulated or relieved stress (e.g., Gupta and Scholz, 2000; see Ch.1: Figure 1.5). These variations in a fault's displacement pattern can determine whether two segments are active independent of each other, or if one fault is influencing the other's movement as part of a larger system (see, e.g., McLeod et al., 2000).

Displacement Profiles Methods

Displacement profiles are made by plotting displacement versus distance along the strike. Here I use previously constructed structure maps acquired from the literature on the faults within the study area, namely Meltzer (1966) and Sabate (1968). The measurements are in terms of throw (or vertical component of displacement) taken by hand directly from their paper maps. The location of the mapped faults is shown in relation to the study area in Figure 3.12.

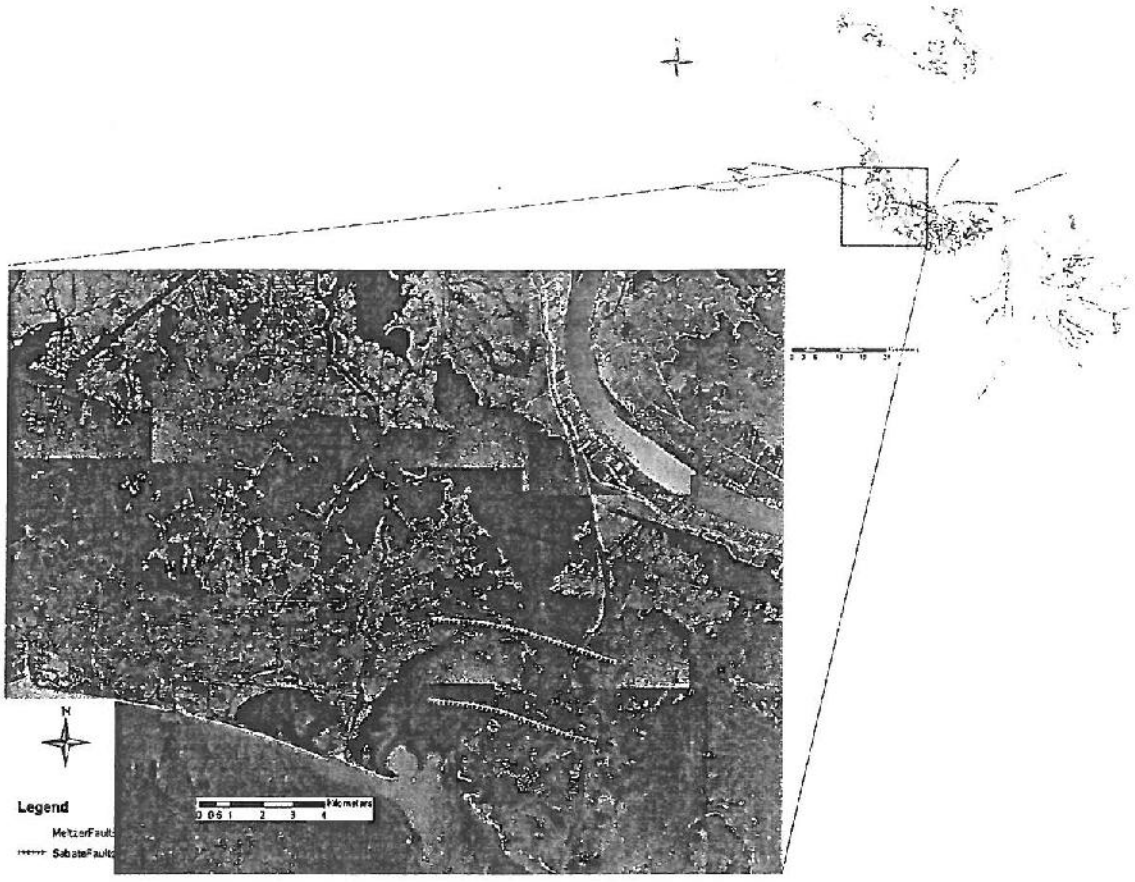

Figure 3.12. Location of the faults mapped by Meltzer (1966) and by Sabate (1968) and close up in the immediate area of interest.

Displacement Profiles Results

The Meltzer profiles do not include data from Meltzer's fault "A" (Fig 3.13) as the depth of the footwall are not recorded on his map. This is unfortunate because fault "A", with it's large displacement (up to 1000 meters of throw according to the Meltzer's text) and coincidental placement, is likely to be the Bastian Bay fault observed in the paper seismic and the well log data discussed above. Fault "B" (Fig 3.13) is therefore interpreted as the smaller outboard fault observed in the onshore seismic sections. Its profile is still interesting because in the deeper sections the displacement begins to increase again toward the east, probably due to the appearance of an unlabeled fault at the eastern tip of Fault "B". All mapped sands used here from Meltzer (1966) are in the upper Miocene.

The Sabate (1968) displacement profiles are useful despite the absence of detailed data over the exact area of the Empire fault (Fig 3.14). However, the profiles to the east and west of the Empire marsh break area provide relevant information. The western fault segments show a multi-segment pattern with the smaller interacting segments skewed towards one another. The overall displacement of these segments, taken as one linked fault, is skewed toward the east. The displacement then begins to increase again toward the east. Here there is a gap in the data with the immediate area of the Empire fault labeled as "not contoured" on Sabate's (1968) published map. The segment profile to the east of the data gap is skewed towards the west where the Empire fault is inferred to be. Faults from Sabate (1968) were mapped at the basal Pleistocene sand and show almost 150 m of displacement.

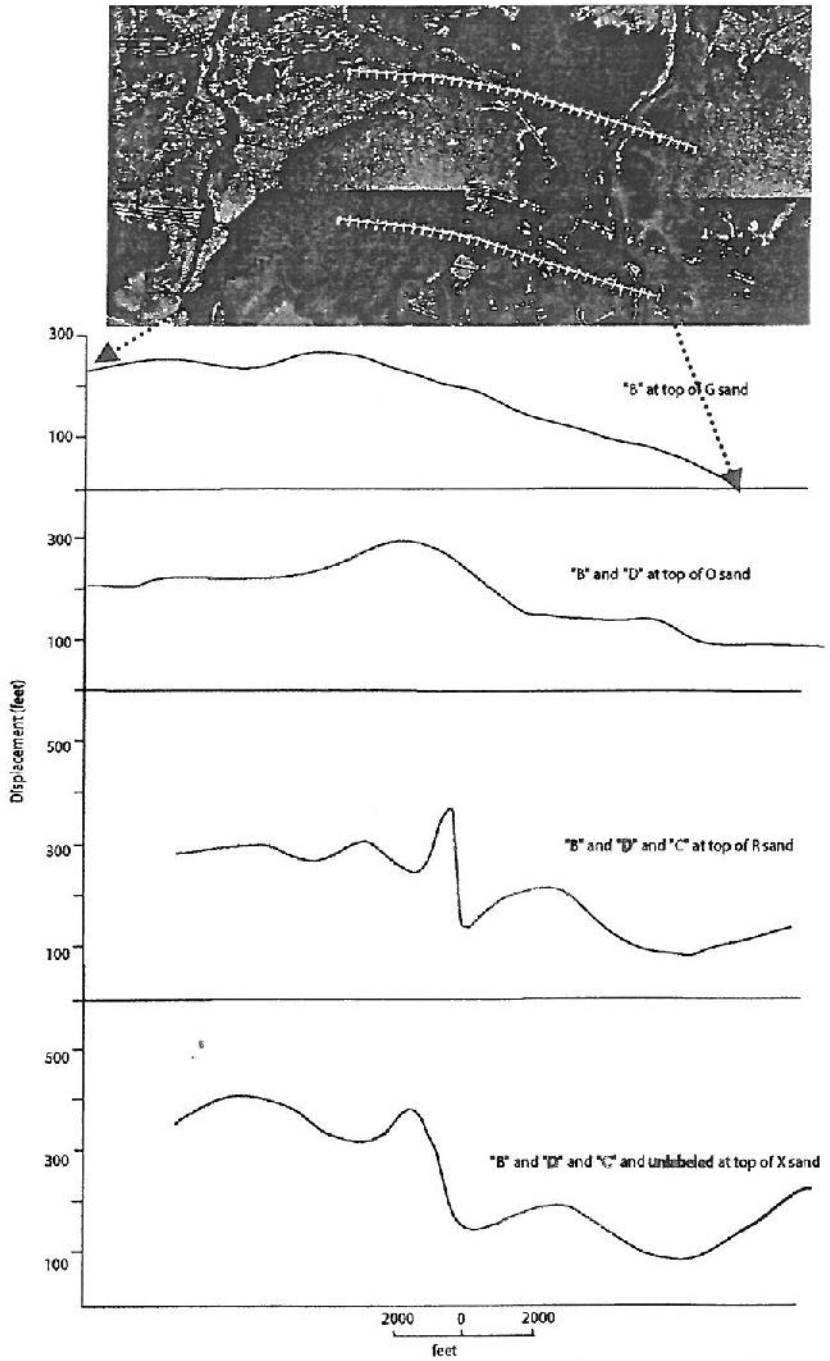

Figure 3.13. Displacement profiles constructed from Meltzer (1968), plotted in terms of throw (or vertical displacement). The southernmost of the two faults marked in yellow above is Meltzer's fault "B". The northernmost fault marked on the DOQQs in this figure is Meltzer's fault "A" and was mapped with data gaps that did not allow for it to be included in the calculated displacement profiles. It is, however, mapped as a larger fault with generally more displacement than the other faults shown here combined. The other faults referred to in the profiles ("C", "D", and "unlabeled") are in the immediate vicinity of fault "B".

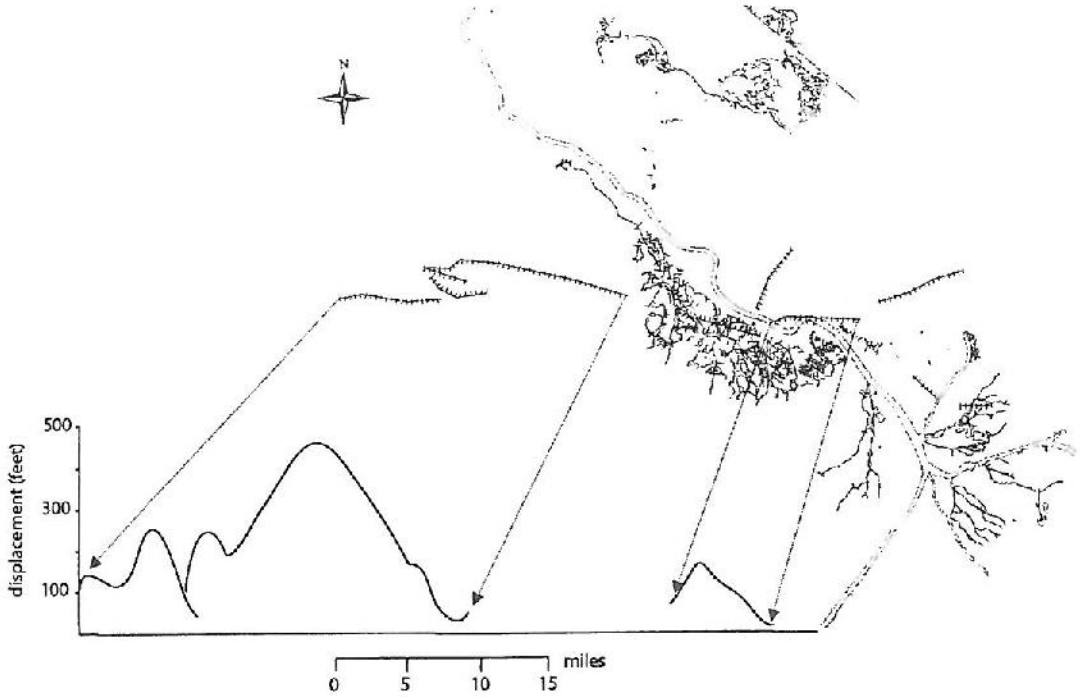

Figure 3.14. Displacement profiles, plotted in terms of throw, for the south dipping faults mapped by Sabate (1968). All blue faults are from Sabate (1968) and yellow from Meltzer (1966). The fault shown in blue in between the two areas of calculated displacement is an antithetic fault. The slight increase in displacement on the eastern mapped end of the western group of segments and the skewed profile of the easternmost segment suggest the existence of another interacting fault segment.

Displacement Profiles Discussion & Summary

The faults mapped by Meltzer (1966) and Sabate (1968) coincide with those analyzed in this study. There is a data gap in the area of the Empire fault, however Sabate maps a large, east-west striking, south-dipping fault along the same latitude to the west of the Empire marsh break. This could be another segment in this system. The Bastian Bay fault is also absent, but there does appear to be a north-dipping fault just north of, and parallel to, the Bastian Bay marsh breaks. The placement and dip suggest this could be the antithetic fault interpreted in onshore seismic line "C" (Fig 3.10).

The displacement profiles of these south-dipping segments mapped by Sabate (1968), to the east and west of the Empire fault, support the presence of the Empire fault by both their skewed profiles and the beginning of what may be the Empire segment observed at the eastern edge of the western fault segments. Figure 3.12 shows that the end of the mapped western fault segments corresponds to the beginning of the marsh break area at Empire.

While the profiles of Meltzer's (1966) faults are of limited use due to the absence of contour data for fault "A^{1}", which is likely the Bastian Bay fault, the map itself corroborates the interpretation put forth in this thesis for the Bastian Bay fault. The two faults mapped at depth by Meltzer (1966) that are located just south of, and parallel to, the Bastian Bay marsh break correlate well with the two faults in seismic lines "A" and "B" (see section above, Figs. 3.8 & 3.9). The northernmost, or inboard, of the two faults being the Bastian Bay fault, which is here proposed to reach the surface. While the displacement profiles from Meltzer's mapping (1968) do show the largest displacement to the west, this does not contradict the higher displacement observed to the east as

interpreted from the paper seismic (discussed in the "Onshore Seismic" section above). This is because Meltzer's dataset does not extend as far to the east as line "C" (For location of Line "C" see Figure 3.7).

It is interesting to note that the footwall contours of Fault "A" are likely not recorded because the purpose of Meltzer's (1966) study was to focus on the structures as they relate to the West Bastian Bay gas field, which is located on the downthrown, or hanging wall section of the large fault. This is interesting in terms of possible fault re-activation triggers. This field produced large amounts of oil and gas in the 1960s (according to Meltzer, in 1965 it was responsible for 2.1 billion cubic meters of gas, 573,000 barrels of condensate, and 566,000 barrels of oil.). Although by the 1970's its production of natural gas had begun to decline, production was still reported in the millions of cubic meters per year until 2000 when the field's output declined again significantly. Barrels of oil in the six figures per year were reported until the year 2005 when production dropped precipitously (according to the La. DNR SONRIS database, SRCN2729 field production PDF).

This field was producing from sands within the upper Miocene. This fits expansion index interpretations of the well data above. At the time when the fault was most active, the most expansion would take place, building up thick sand beds for future reservoirs. Oil and gas withdrawal has been associated with subsidence throughout southern Louisiana (Morton et. al., 2002). Is the correlative also causative, and if so, is it relevant in the particular case of Bastian Bay? If the data were available, comparing the fine scale kinematics of the more recent fault movement to the production history of the

nearby gas fields may help to either confirm or disprove the hypothesis that human activities, such as fluid withdrawal, are influencing faulting and subsidence.

CHAPTER 4: DISCUSSION AND CONCLUSIONS

Summary

This study confirms the existence of two large, coast-parallel normal faults near Empire and Bastian Bay, Louisiana: the "Empire fault", and the "Bastian Bay fault". The surface data (e.g., aerial imagery of land loss over time, auger cores, and bathymetric profiles) shows these faults to be both mappable and active at the surface. The auger cores combined with the radiocarbon dating suggest that there has been movement along the Empire fault in post ca.770 AD sediments (Figure 2.6). These sediments show up to a meter of vertical offset. The very recent marsh loss (as concluded from historical photos) along these faults indicates activity within the past few decades (Figure 2.2). Furthermore, variations in displacement observed along the Empire fault indicate that the fault does not die out at the ends of the segments that make up the visible marsh break, but continues both to the east and to the west of the field area.

From subsurface data, there is further evidence of two faults in the study area and their recent (Pleistocene-Holocene) activity. With subsurface data I expand the kinematic history of both faults. The correlation of local well logs and interpretation of seismic data reveals two major, coast-parallel growth faults, which correspond in space with the observed surface faults. The well log data shows the Empire fault continuing to the east, as predicted by the auger core data, and reinforces the conclusion that movement along the Empire fault must have occurred recently (late Pleistocene to Holocene). The Bastian

Bay fault is also shown to have been active sometime between the early Pleistocene and Holocene. The expansion indices calculated from the well log data show at least two periods of activity along both of these faults: the more recent period mentioned above and an earlier period in the Miocene.

The onshore seismic lines reveal the same kinematics as seen in the well log correlation and, with the shotpoint data, narrow down the point at which the subsurface faults intercept the surface. This confirms that the Empire and Bastian Bay faults seen at the surface marsh break are the surface expression of the two faults seen in all the subsurface data. A first order calculation of displacement profiles using the seismic data suggests that it is likely the Bastian Bay fault (like the Empire fault) continues to the east of its surface expression (Fig 3.11). The Empire fault is interpreted to cross the Mississippi River. Given these findings, along with the population of faults similar in size, kinematics and structure to the Empire and Bastian faults observed to the east of the Mississippi River in the offshore seismic data, it is critical to complete studies similar in nature to this one along the river and the levee system at this latitude.

How, directly, the Empire and Bastian Bay faults relate to previously mapped regional faults is still ambiguous. To answer that question the results presented herein must be expanded to cover the gap between Empire and the faults offshore to the east, as well as to the west between Lake Washington and the section of the Golden Meadow fault that has been well-established just north of Lake Felicity (Kuecher, 1994). Although Kuecher (1994) reports considerable detail about the faults in the Lake Felicity area no kinematic analyses that could be compared to this study have been published. The

question of whether the Empire and/or Bastian Bay fault are the western segments of the Golden Meadow fault remains open.

The results presented here do show that the hypothesis that the Empire and the Bastian Bay fault segments represent simple en echelon segments near the eastern tip of the overall Golden Meadow fault trend is overly simplistic. However, the fact that the faults in this study both appear to have displacement that postdates deposition of the upper few 100 meters of sediment, both have documented historic subsidence, and both show similar past movement in the Miocene, does suggest that they may be part of the same fault system. Due to the large displacements at depth where they overlap, they would likely not be considered simple en echelon segments of the same fault. Studying additional seismic lines along the Golden Meadow fault and compilation of expansion indices (i.e., was there also a period of activity in the Miocene?) would prove useful in related the two systems.

Implications

A growing body of work consisting of modeling, surface observations, and subsurface data supports the notion of active faulting in southern Louisiana (e.g. Gagliano, 1999; Morton et al, 2001; Kuecher et. al., 2001; Dokka, 2006). This is in addition to previous subsurface work that proves the existence of large faults throughout the region (e.g. Meltzer, 1966; Sabate, 1968; Bebout et al., 1983). This study adds to both of these bodies of work and further synthesizes the subsurface and surface data for a particular area. While there are many explanations for subsidence along the gulf coast, the bulk of the evidence presented here points to spatially varying subsidence and subsequent land loss in Empire and Bastian Bay being caused by faulting.

It is important to note that this may not hold true for surrounding areas. Faulting did not cause every acre of marsh that falls below sea level in Louisiana (e.g., Barataria Bay; see reference to Wilson in Chapter 2). The initial clue is the pattern of marsh breaks. If they are linear and slightly arcuate in nature, then further investigation into faulting is warranted. If the pattern of loss does not immediately suggest faulting then the investigation should focus on local differential compaction rates, human activity such as dredging and fluid withdrawal, and storm-induced marsh edge erosion.

Although this investigation of land loss near Empire and in Bastian Bay began with surficial observations that suggested faulting, there are other ways to approach the initial question of which areas of subsidence involve tectonics. This is addressed by both Dokka (2006) and Meckel et. al. (2006). Dokka (2006) shows that faulting can be a major cause of subsidence, even in areas without obvious geomorphic manifestations. Dokka (2006) looks specifically at teasing out the various contributors to subsidence in a specific area. He shows how, in the Michoud area of eastern New Orleans, some of the subsidence originates far below the surface (>2000 m or middle Miocene to Jurassic) and is likely of faulting origin. This fault related subsidence peaked between 1969 and 1971, tapering off thereafter and disappearing by 2005. Dokka hypothesizes that the portion of the subsidence not accounted for by deep or fault strain is due to both compaction in the intermediate (Pleistocene to middle Miocene) sediments, and to various processes at work in the upper 200 m (Holocene to Pleistocene) of strata. The recent reactivation of a Miocene fault discussed in the aforementioned paper may be compared to the history proposed in this thesis for the Empire area. Meckel et al (2006) derives a process in

which the likely amount of Holocene compaction can be calculated. If subsidence rates are much higher than this, the probability of other factors, possibly tectonic, increases.

If faulting is a widespread mechanism that results in subsidence and land loss, what is the cause? Have the fault triggers been established? After Morton (2001) proposed fault reactivation in several hydrocarbon fields of southern Louisiana coincident with times of high oil and gas production, Chan (2004) analyzed the releveling surveys on which Morton based his work. He also modeled fault displacements to determine if movement along the local segment of the Golden Meadow fault system in the Lapeyrouse field could produce the observed subsidence pattern. While Chan (2004) shows this to be a reasonable assessment (general field-wide subsidence with an area of increased subsidence along the hanging wall of the fault where the field produced from the rollover area) all fault movement is local to the field or in a small area of deformation around the immediate area of withdrawal. This suggests that the "fault movement" seen around the fields is not traditionally understood slip of the fault but, instead, is preferential compaction on the hanging wall side of the fault. In some cases the amount of subsidence along the Golden Meadow fault cannot be fully explained by local withdrawal compaction. Using the numerical fault mechanics program Poly3D, Chan (2004) shows how the fault may be encouraged to actually slip due to the reservoir compaction. He concludes from this that the compaction due to fluid withdrawal from the reservoir may affect the stresses around the fault enough to either hasten or postpone slip events on the active growth fault (Chan, 2004).

In contrast to the Lapeyrouse field along the Golden Meadow fault, the recent subsidence at the Empire marsh breaks is not immediately coincident with any large

hydrocarbon withdrawal (Figure 1.2). However, as discussed in Chapters 2 and 3 and above, these breaks are likely just the visible section of larger fault segments that extend to the east and west. If this is the case, one might speculate that areas of oil and gas production farther east or west along this fault systems may have been involved in the stress changes that eventually, through segment interaction, lead to movement along the Empire segments. In Bastian Bay, comparing the timing and physical extent of subsidence with the production history of the Bastian Bay gas fields may help determine if local fault movement was directly or indirectly affected by industry activity. Even if a connection can be made between historic subsidence and fluid withdrawal in Bastian Bay, the kinematics of the Bastian Bay fault and the Empire fault presented in this study clearly show that these faults were reactivated in the Pleistocene-Holocene, not just in the past few decades. If industry activity is affecting the most recent fault movements in the area, it should be considered an overprint on a much more extensive period of fault activity whose triggering mechanism remains unknown.

Future work

As seen above, any discussion of current research on the causes and processes of, and solutions to, subsidence and land loss in southern Louisiana begs more questions than it answers. Generally, the methods used in each of the studies mentioned above (fieldwork, geodetic leveling, subsurface investigations and modeling) all need to be expanded to cover all areas of potentially tectonic subsidence.

More specifically, stemming directly from this study and with short-term mitigation and disaster prevention in mind, the comprehensive techniques of this study should be extended to include the area immediately surrounding the Mississippi River.

The present importance of this river commercially demands that we take the possibility of an active fault crossing it, and the storm and river protection levees that surround it, seriously. Based on the conclusions presented throughout this paper, the faults observed at Empire and Bastian Bay most likely continue to the east. Additional evidence of faulting may be detectable along the Mississippi River in Plaquemines Parish. Geodetic work along the levees just east of Empire and Bastian Bay and correlations based on shallow to intermediate borings to determine any local offsets is advisable. These two areas of future study should help determine the placement and timing of faulting events. Intermediate depth borings would aid in covering the data gap that exists between the data collected with auger cores and vibracores (top few meters to tens of meters) and the geophysical data collected in the deeper subsurface (below 200-700 meters).

Besides collection of new data, the detailed kinematics of the faults presented here should be more thoroughly investigated. If the required data could be obtained, the TWTT of the seismic lines should be converted into depth. This along with stratigraphic marker data from wells could accurately pinpoint the timing of the major faulting cycles seen here. This combination of surface traces of recent faulting and subsurface studies of fault histories should continue to be applied to the entire Louisiana coastal region.

BETA

BETA ANALYTIC INC.

DR. M.A. TAMERS and MR. D.G. HOOD

UNIVERSITY BRANCH
4985 S.W. 74 COURT
MIAMI, FLORIDA, USA 33155
PH: 305/667-5167 FAX: 305/663-0964
E-MAIL: beta@radiocarbon.com

REPORT OF RADIOCARBON DATING ANALYSES

Dr. Emily Martin

Report Date: 2/25/2005

Tulane University

Material Received: 1/25/2005

Sample Data	Measured Radiocarbon Age	13C/12C Ratio	Conventional Radiocarbon Age(*)
Beta - 200997 SAMPLE : EMPIRET1C201 ANALYSIS : AMS-Standard delivery MATERIAL/PRETREATMENT : (peat): acid/alkali/acid 2 SIGMA CALIBRATION : Cal AD 1030 to 1240 (Cal BP 920 to 710)	910 +/- 40 BP	-26.0 o/oo	890 +/- 40 BP
Beta - 200998 SAMPLE : EMPIRET2C303 ANALYSIS : AMS-Standard delivery MATERIAL/PRETREATMENT : (peat): acid/alkali/acid 2 SIGMA CALIBRATION : Cal AD 1290 to 1410 (Cal BP 660 to 540)	570 +/- 40 BP	-21.8 o/oo	620 +/- 40 BP
Beta - 200999 SAMPLE : EMPIRET3C205 ANALYSIS : AMS-Standard delivery MATERIAL/PRETREATMENT : (peat): acid/alkali/acid 2 SIGMA CALIBRATION : Cal AD 1430 to 1520 (Cal BP 520 to 430) AND Cal AD 1580 to 1630 (Cal BP 380 to 320)	200 +/- 40 BP	-12.0 o/oo	410 +/- 40 BP
Beta - 201000 SAMPLE : EMPIRET3C307 ANALYSIS : AMS-Standard delivery MATERIAL/PRETREATMENT : (peat): acid/alkali/acid 2 SIGMA CALIBRATION : Cal AD 1030 to 1230 (Cal BP 920 to 720)	880 +/- 40 BP	-23.9 o/oo	900 +/- 40 BP
Beta - 201001 SAMPLE : EMPIRET4C108 ANALYSIS : AMS-Standard delivery MATERIAL/PRETREATMENT : (peat): acid/alkali/acid 2 SIGMA CALIBRATION : Cal AD 1020 to 1210 (Cal BP 930 to 740)	920 +/- 40 BP	-24.7 o/oo	920 +/- 40 BP

Dates are reported as RCYBP (radiocarbon years before present, "present" = 1950A.D.). By international convention, the modern reference standard was 95% of the C14 content of the National Bureau of Standards' Oxalic Acid & calculated using the Libby C14 half life (5568 years). Quoted errors represent 1 standard deviation statistics (68% probability) & are based on combined measurements of the sample, background, and modern reference standards.

Measured C13/C12 ratios were calculated relative to the PDB-1 international standard and the RCYBP ages were normalized to -25 per mil. If the ratio and age are accompanied by an (*), then the C13/C12 value was estimated, based on values typical of the material type. The quoted results are NOT calibrated to calendar years. Calibration to calendar years should be calculated using the Conventional C14 age.

BETA ANALYTIC INC.
DR. M.A. TAMERS and MR. D.G. HOOD
UNIVERSITY BRANCH
4985 S.W. 74 COURT
MIAMI, FLORIDA, USA 33155
PH: 305/667-5167 FAX: 305/663-0964
E-MAIL: beta@radiocarbon.com

REPORT OF RADIOCARBON DATING ANALYSES

Dr. Emily Martin

Report Date: 2/25/2005

Sample Data	Measured Radiocarbon Age	13C/12C Ratio	Conventional Radiocarbon Age(*)
Beta - 201002 SAMPLE : EMPIRET4C210 ANALYSIS : AMS-Standard delivery MATERIAL/PRETREATMENT : (peat): acid/alkali/acid 2 SIGMA CALIBRATION : Cal AD 1400 to 1450 (Cal BP 550 to 500)	530 +/- 40 BP	-26.0 o/oo	510 +/- 40 BP
Beta - 201003 SAMPLE : EMPIRET4C311 ANALYSIS : AMS-Standard delivery MATERIAL/PRETREATMENT : (charred material): acid/alkali/acid 2 SIGMA CALIBRATION : Cal AD 1020 to 1210 (Cal BP 930 to 740)	790 +/- 40 BP	-17.1 o/oo	920 +/- 40 BP
Beta - 201004 SAMPLE : EMPIRET5C112 ANALYSIS : AMS-Standard delivery MATERIAL/PRETREATMENT : (peat): acid/alkali/acid 2 SIGMA CALIBRATION : Cal AD 970 to 1040 (Cal BP 980 to 910)	1020 +/- 40 BP	-25.1 o/oo	1020 +/- 40 BP
Beta - 201005 SAMPLE : EMPIRET5C417 ANALYSIS : AMS-Standard delivery MATERIAL/PRETREATMENT : (charred material): acid/alkali/acid 2 SIGMA CALIBRATION : Cal AD 770 to 970 (Cal BP 1180 to 980)	1200 +/- 40 BP	-26.3 o/oo	1180 +/- 40 BP

Dates are reported as RCYBP (radiocarbon years before present, "present" = 1950A.D.). By international convention, the modern reference standard was 95% of the C14 content of the National Bureau of Standards' Oxalic Acid & calculated using the Libby C14 half life (5568 years). Quoted errors represent 1 standard deviation statistics (68% probability) & are based on combined measurements of the sample, background, and modern reference standards.

Measured C13/C12 ratios were calculated relative to the PDB-1 international standard and the RCYBP ages were normalized to -25 per mil. If the ratio and age are accompanied by an (*), then the C13/C12 value was estimated, based on values typical of the material type. The quoted results are NOT calibrated to calendar years. Calibration to calendar years should be calculated using the Conventional C14 age.

LIST OF REFERENCES

Autin, W.J., Burns, S.F., Miller, B.J., Saucier, R.T., and Snead, J.I., 1991, Quaternary geology of the lower Mississippi Valley: Geol. Soc. Amer., Decade of North American Geology, Quaternary Nonglacial Geology: Conterminous U.S., v. K-2, p. 547-582

Autin, W.J., 1993, Influences of relative sea-level rise and Mississippi River delta plain evolution on the Holocene middle Amite River, Southeastern Louisiana: Quaternary Research, v. 39, p. 68-74

Bebout, D.G., and Gutierrez, D.R., 1983, Regional cross-sections Louisiana gulf coast eastern part: Louisiana Geological Survey, Folio Series, no. 4, p. 1-10

Bou-Rabee, F., 1994, Earthquake recurrence in Kuwait induced by oil and gas extraction: Journal of Petroleum Geology, v. 17, no. 4, p. 473-479

Cartwright, J., Bouroullec, R., James, D., and Johnson, H., 1998, Polycyclic motion history of some Gulf Coast growth faults from high-resolution displacement analysis: Geology, v. 26, p. 819-22.

Chan, A., 2004, Production-induced reservoir compaction, permeability loss and land surface subsidence: Chapter 5: Louisiana coastal wetland loss: the role of hydrocarbon production: Dissertation Thesis, Stanford University, p. 88-135

Coleman, J.M., Roberts, H.H., and Stone, G.W., 1998, Mississippi river delta: an overview: Journal of Coastal Research, v. 14, no. 3, p. 698-716

Cowie, P.A., and Shipton, Z.K., 1998, Fault tip displacement gradients and process zone dimensions: Journal of Structural Geology, v. 20, n. 8, p. 983-997

Cowie, P. A., Gupta, S., and Dawers, N.H., 2000, Implications of fault interaction for early syn-rift sedimentation: insights from a numerical fault growth model: Basin Research, v. 12, p. 241-262

Cowie, P.A., and Scholz, C.H., 1992, Physical explanation for displacement-length relationship for faults using a post-yield fracture mechanics model: Journal of Structural Geology, v. 14, p. 1133-1148

Dawers, N.H., Anders, M.H., and Scholz, C.H., 1993, Growth of normal faults: displacement-length scaling: Geology, v. 21, p. 1107-1110

Diegel, F.A., Karlo, J.F., Schuster, D.C., Shoup, R.C., and Tavers, P.R., 1996, Cenozoic structural evolution and tectono-stratigraphic framework of the Northern Gulf Coast continental margin: Salt Tectonics: a global perspective, edited by Jackson, M.P.A., Roberts, D.G., and Snelson., S.

Dokka, R.K., 2005, Geological implications of recently derived vertical velocities of benchmarks of the south-central United States of America: Eos, Transactions of the American Geophysical Union Joint Assembly Supplement, Abstracts, v. 86, no. 18, G43A-01

Dokka, R.K., 2006, Modern-day tectonic subsidence in coastal Louisiana: Geology, v. 34, P. 281-284

Durham, C.O. and Peeples, E.M., 1956, Pleistocene fault zone in southeastern Louisiana: Transactions of the Gulf Coast Association of Geological Societies, v. 6, p. 65-66

Ervin, C.P., and McGinnis, L.D., 1975, Reelfoot Rift: reactivated precursor to the Mississippi embayment: Geological Society of America Bulletin, v. 86, no. 9, p. 1287-1295

Fisk, H. N., 1944, Geological investigation of the alluvial valley of the lower Mississippi river, Vicksburg, MS: U. S. Army Corps of Engineers, Mississippi River Commission.

Gagliano, S.M., 1999, Faulting, subsidence and land loss in coastal Louisiana: Coast 2050: Toward a sustainable coastal Louisiana, The Appendices. Louisiana Department of Natural Resources, Baton Rouge, La. 47.

Gagliano, S.M., 2002, unpublished data

Gagliano, S.M., Kemp, E.B., III, Wicker, K.M., and Wiltenmuth, K.S., 2003a, Active geological faults and land change in southeastern Louisiana: Report to the US Army Corps of Engineers, New Orleans District, April 2003.

Gagliano, S.M., Haggar, K., Kemp E.B., III, McCulloh, R.P., and Sabate, R., 2003b, The Baton Rouge fault system: A model for coastal land loss. 2003: Field Trip # 4 Guidebook, Annual Convention of the Gulf Coast Association of Geological Societies and the Gulf Coast Section, SEPM, p. 1-62

Galloway, W.E., Ganey-Curry, P.E., Li, X., and Buffler, R.T., 2000, Cenozoic depositional history of the Gulf of Mexico basin: American Association of Petroleum Geologists, v. 84, p. 1743-1774

Galloway, W.E., 2001, Cenozoic evolution of sediment accumulation in deltaic and shore-zone depositional systems, northern Gulf of Mexico basin: Marine and Petroleum Geology, v. 18, p. 1031-1040

Gupta, A., and Scholz, C.H., 2000, A model of normal fault interaction based on observations and theory: Journal of Structural Geology, v. 22, p. 865-879

Hanor, J.S., 1982, Reactivation of fault movement, Tepetate fault zone, south central Louisiana: Transactions – Gulf Coast Association of Geological Societies. v. 32, pp. 237-245

Hardin, F.R., and Hardin. G.C., 1961, Contemporaneous normal faults of the gulf coast and their relation to flexures: American Association of Petroleum Geologists Bulletin, v. 45, p. 238-248

He, L., Dawers, N., and Stelting, C., 2006, Post-30-M.y. sequence stratigraphy, northeastern Gulf of Mexico: AAPG Annual Meeting, April 9-12, Houston, Tx.

Heinrich, P.V., 2000, De Quincy fault-line scarp, Beauregard and Calcasieu parishes, La.: Basin Research Institute Bulletin, v. 9, p. 38-50

Hildenbrand, T.G., 1985, Rift structure of the northern Mississippi embayment from the analysis of gravity and magnetic data (USA): Journal of Geophysical Research, v. 90, no. B14, p. 12607-12622

Holbrook P.W., Maggiori, D.A., and Hensley, R., 1995, Real-time pore pressure and fracture-pressure determination in all sedimentary lithologies: SPE Formation Evaluation, v. 10, no.4, p. 215-222

Jurkowski, G., Ni, J., and Brown, L., 1984, Modern uparching of the gulf coastal plain: Journal of Geophysical Research, v. 89, no. B7, p. 6247-6255

Kane, M.F., Hildenbrand, T.G., and Hendricks, J.D., 1981, Model for the tectonic evolution of the Mississippi embayment and its contemporary seismicity: Geology, v. 9, no. 12, p. 563-568

Kosters, E.C., 1989, Organic-clastic facies relationships and chronostratigraphy of the Barataria interlobe basin, Mississippi delta plain: Journal of Sedimentary Petrology, v. 59, no. 1, p. 98-113

Kuecher, G.J., Roberts, H.H, Thompson, M.D., and Matthews, I., 2001, Evidence for active growth faulting in the Terrebonne delta plain, south Louisiana: Implications for wetland loss and the vertical migration of petroleum: Environmental Geosciences, v. 8, p. 77-94

Kulp, M.A., Howell, P.D., Adiau, S., Penland, S., Kindinger, J.L., and Williams, S.J., 2002, Latest quaternary stratigraphic framework of the Mississippi river delta region: Gulf Coast Association of Geological Societies and Gulf Coast Section SEPM: technical papers and Abstracts: Dutton, S.P., et al. Eds.: Transactions, v. 52, p. 573-582

Lowrie, A, MacKenzie, M.G., Guderion, E., and Talbert, F.E., 1997, Sedimentary shattering as hydrocarbon migration avenues in salt-floored basins: a new migration paradigm: Energy Exploration and Exploitation, v. 15, no. 4-5, p. 387-395

Lowrie, A., 1986, Model for fine-scale movements associated with climate and sea level changes along Louisiana shelfbreak growth faults: Transactions - Gulf Coast Association of Geological Societies, v. 36, p. 497-509

Mauduit, T., and Brun, J.P., 1998, Growth fault/rollover systems: Birth, growth, and decay: Journal of Geophysical Research, v. 103, no. B8, p. 18119-18136

McCulloh, R.P., 1994, Sediment intervals and correlative hiatuses associated with growth faults: an overview of published examples: Louisiana Geological Survey, Baton Rouge, Open-File Series no. 94-01

McCulloh, R.P., 1996, Surface faults in East Baton rouge parish: Louisiana Geological Survey, Baton Rouge, Open-File Series no. 91-02

McLeod, A.E., Dawers, N.H., and Underhill, J.R., 2000, The propagation and linkage of normal faults: insights from the Strathspey-Brent-Statfjord fault array, northern North Sea: Basin Research, v. 12, p.263-284

Meckel, T.A., ten Brink, U.S., and Williams, S.J., 2006, Current subsidence rates due to a compaction of Holocene sediments in southern Louisiana: Geophysical Research Letters, v. 33, L11403

Meltzer, L.H., 1966, The geology of the West Bastian Bay field Plaquemines parish, La.: Transactions – Gulf Coast Association of Geological Societies, v. 16, p. 199-210

Mooney, W.D., Andrews, M.C., Ginzburg, A., Peters, D.A., and Hamilton, R.M., 1983, Crustal structure of the northern Mississippi embayment and a comparison with other continental rift zones: Tectonophysics, v. 94, no. 1-4, p. 327-348

Morton, R.A., Buster, N.A., and Krohn, M.D., 2002, Subsurface controls on historical subsidence rates and associated wetland loss in south-central Louisiana: Transactions - Gulf Coast Association og Geological Societies, v. 52, p. 767-778

Morton, R.A. and Purcell, N.A., 2001, Wetland subsidence, fault reactivation, and hydrocarbon production in the U.S. Gulf Coast region: USGS Fact Sheet, FS-091-01

Nunn, J.A, 1985, State of stress in the northern gulf coast: Geology, v. 13, p. 429-432

Ocamb, R.D., 1961, Growth faults of South Louisiana: Transactions - Gulf Coast Association of Geological Societies, v. 11, p. 139-175

Penland, S., Wayne, L., Britsch, L.D., Williams, S.J., Beall, A.D., and Butterworth, V.C., 2000, Geomorphic classification of coastal land loss between 1932 and 1990 in the Mississippi river delta plain, Southeastern Louisiana: USGS, Open File Report 00-417

Sabate, R.W., 1968, Pleistocene oil and gas in Louisiana: Transactions - Gulf Coast Association of Geological Societies, v. 18, p. 373-386

Saucier, R.T., 1963, Recent geomorphic history of the Pontchartrain basin. Baton Rouge, La.: Louisiana State University Press.

Saucier, R.T., 1994, Geomorphology and quaternary geologic history of the lower Mississippi Valley: U.S. Army Corps of Engineers, Vicksburg Mississippi, v. I

Sella, G.F., Dokka, R.K., Dixon, T.H., and Hossain, I., 2005, Present-day deformation along the Northern Gulf of Mexico as observed by continuous and episodic GPS observation: Eos, Transactions American Geophysical Union, Joint Assembly Supplementary Abstracts, v. 86, no. 18, G43A-03

Serebryakov, V.A., and Chilingar, G.V., 2000, Prediction of subsidence: relationship between lowering of formation pressure and subsidence due to fluid withdrawal: Energy Sources. v. 22, p. 409-416

Shinkle, K.D., and Dokka, R.K., 2004, Rates of vertical displacement st benchmarks in the lower Mississippi valley and the northern gulf coast: NOAA Technical Report, NOS/NGS 50

Spearing, D., 1995, Roadside geology of Louisiana: Mountain Press Publishing Co.

Spitz, W.J., and Schumm, S.A., 1997, Tectonic geomorphology of the Mississippi Valley between Osceola, Arkansas and Friars Point, Mississippi: Engineering Geology, v. 46, no.3-4, p. 259-280

Tearpock, D.J., and Bischke, R.E., 2002, Applied Subsurface Geological Mapping with Structural Methods (2nd Edition): Prentice Hall PTR, p. 1-864

Thorsen, C.E., 1963, The age of growth faulting in Southeast Louisiana: Transactions – Gulf Coast Association of Geological Societies, v. 13, p. 103

White, W.A., and Morton, R.A., 1997, Wetland losses related to fault movement and hydrocarbon production, southeastern Texas coast: Journal of Coastal Research, v. 13, no. 4, p. 1305-1320

Wilson, C.A., Allison, M.A., 2006, Sediment dynamics and geomorphology of eroding marsh shorelines in southeastern Louisiana: GSA ann. mtg., 22–25 Oct, no. 96-6

Worrall, D.M., and Snelson. S., 1989, Evolution of the northern Gulf of Mexico, with emphasis on Cenozoic growth faulting and the role of salt: Geology of North America – an Overview, edited by Bally, A.W., and Palmer, A.R., Geological Society of America, Boulder, Colorado, p. 97-138.